General Disclaimer

One or more of the Following Statements may affect this Document

- This document has been reproduced from the best copy furnished by the organizational source. It is being released in the interest of making available as much information as possible.

- This document may contain data, which exceeds the sheet parameters. It was furnished in this condition by the organizational source and is the best copy available.

- This document may contain tone-on-tone or color graphs, charts and/or pictures, which have been reproduced in black and white.

- This document is paginated as submitted by the original source.

- Portions of this document are not fully legible due to the historical nature of some of the material. However, it is the best reproduction available from the original submission.

DOE/NASA/0201-4
NASA CR-168298

Evaluation of Gas-Cooled Pressurized Phosphoric Acid Fuel Cells for Electric Utility Power Generation

Final Technical Report

Mohammad Farooque
Energy Research Corporation

September 1983

Prepared for
NATIONAL AERONAUTICS AND SPACE ADMINISTRATION
Lewis Research Center
Under Contract DEN 3-201

for
U.S. DEPARTMENT OF ENERGY
Fossil Energy
Office of Coal Utilization and Extraction

DOE/NASA/0201-4
NASA CR-168298

Evaluation of Gas-Cooled Pressurized Phosphoric Acid Fuel Cells for Electric Utility Power Generation

Final Technical Report

Mohammad Farooque
Energy Research Corporation
Danbury, Connecticut 06810

September 1983

Prepared for
National Aeronautics and Space Administration
Lewis Research Center
Cleveland, Ohio 44135
Under Contract DEN 3-201

for
U.S. DEPARTMENT OF ENERGY
Fossil Energy
Office of Coal Utilization and Extraction
Washington, D.C. 20545
Under Interagency Agreement DE-AI21-80ET17088

EXECUTIVE SUMMARY

Gas cooling is a more reliable, less expensive and simpler alternative to conventional liquid cooling for heat removal from phosphoric acid fuel cell (PAFC) stacks. The operability of gas cooling has already been demonstrated in atmospheric pressure stacks at current densities of 100 to 150 mA/cm^2. This report presents a theoretical and experimental investigation of gas cooling for a pressurized PAFC operating at current densities in excess of 300 mA/cm^2.

Two different approaches to gas cooling, Distributed Gas (DIGAS) Cooling, and Separated Gas Cooling (SGC) were considered for the pressurized application. A design study to compare various configuration options showed that SGC with a specially designed 'tree' cooling plate, placed every 5 cells in a stack, would provide the best trade-off between cell performance and temperature distribution and cost. A perspective view of such a stack with "Z" type flow passages and 'tree' cooling plates is shown in Figure S-1.

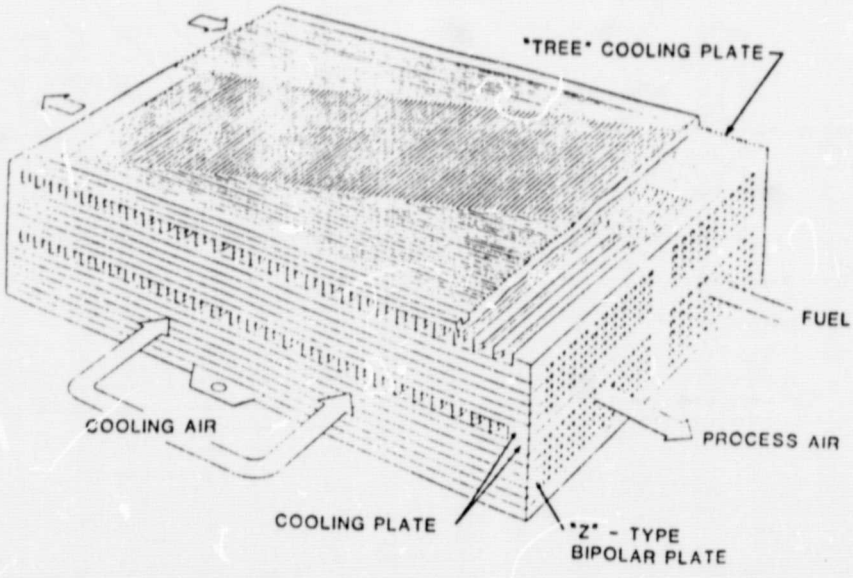

FIGURE S-1 PERSPECTIVE VIEW OF THE SEPARATED GAS-COOLED STACK

The operability of SGC was demonstrated in a proof-of-concept (POC) stack of approximately a 10 kW size, operating at a current density of 325 mA/cm^2 and at pressures between 315 to 690 kPa (45 to 100 psia). The individual cells in the stack were approximately a 1000-cm^2 size, and the average cell temperature was 184°C. An average cell performance of 605 mV/cell was obtained at a pressure of 515 kPa (75 psia). This represents a gain of more than 100 mV/cell over the atmospheric pressure stack. A typical temperature profile in the cell is shown in Figure S-2. As can be seen, a maximum to average temperature difference of ∿11°C is obtained for the above mentioned cooling scheme. Such a temperature gradient appears acceptable from the point of view of cell life and current density distribution. The testing has also pointed to a possible fine tuning of the cooling plate design

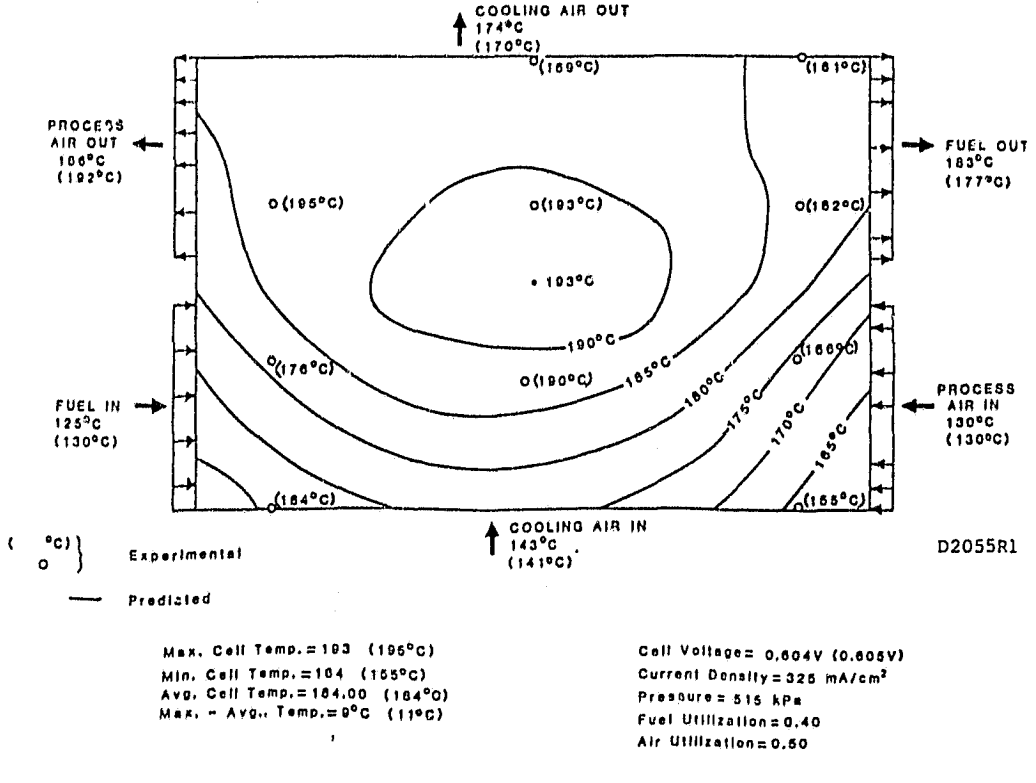

FIGURE S-2 COMPARISON OF PREDICTED AND EXPERIMENTAL TEMPERATURE PROFILE IN A TYPICAL CELL OF 10 kW STACK (The experimental measurements are shown in parantheses)

to further reduce the temperature gradients. Parasitic power corresponding to the coolant and reactant flows through the stack was measured to be very small, <1% of the power output.

The 10 kW stack was operated at various pressures for a total period of 700 hours. During this period, the stack suffered some operational upsets such as a fuel outage and high differential pressures. Performance of the stack, however, remained reasonably stable as shown in Figure S-3. Water balances and performance mapping as a function of various operating variables were also obtained. Data obtained during this mapping would provide valuable design information for the continued development effort on pressurized phosphoric acid fuel cells for utility applications.

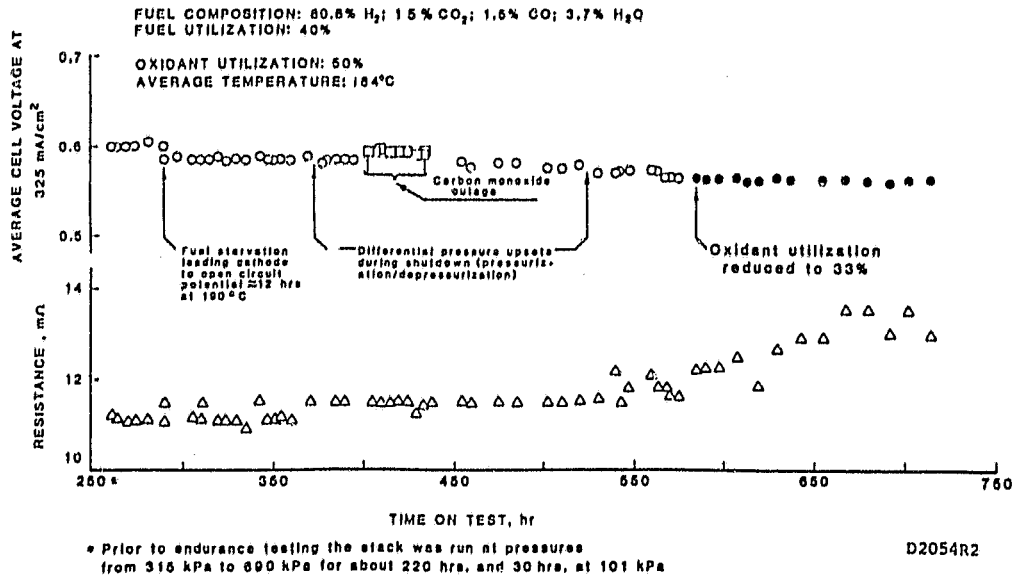

FIGURE S-3 LIFEGRAPH OF THE 10 kW STACK

CONTRIBUTORS

Those who have contributed to the success of this program are acknowledged below:

ERC

J. Ahmad

M. Farooque

M. Hooper

H. Maru

A. Skok

WESTINGHOUSE

R. Harry

R. Kothmann

TABLE OF CONTENTS

TABLE OF CONTENTS (concluded)

INTRODUCTION

The pressurized phosphoric acid fuel cell (PAFC), favored over the atmospheric PAFC because of higher power density and energy conversion efficiency, is being developed for utility power generation (1) under the sponsorship of the Department of Energy, Electric Power Research Institute and the Electric Utilities. The PAFC produces approximately equal amounts of heat and electricity. A steady state operation is ensured through continuous cooling. As is the case with many types of powerplants, cooling is an important system consideration for the PAFC system as well. The various cooling concepts being investigated include two-phase water, alternate dielectric liquid, and gas cooling (2). Among the alternatives, gas cooling appears to be the most reliable, simple, and cost effective approach (1,2,3).

Possible schemes of implementing gas cooling include the distributed gas (DIGAS) cooling scheme (4) and a separated gas cooling (SGC) scheme (5). The former involves a splitting of the process and cooling gas in the same manifold using a properly designed cooling plate and cell passages (Figure 1). Only four gas manifolds are required in this case and the cell passage geometry is simple. The latter scheme as shown in Figure 2, requires six manifolds and a somewhat complex cell passage design. The engineering feasibility of these gas cooling schemes for an atmospheric pressure PAFC has been successfully demonstrated (6). The present study implemented the gas cooling in pressurized fuel cell stacks and demonstrated the engineering feasibility of gas cooling schemes for the pressurized PAFC stacks up to approximately a 10 kW size. The effect of operating variables (temperature, stoichiometric flow rate of reactants, etc.) on performance, parasitic power requirements, CO_2 and CO related performance loss, gas cooling effectiveness, and the need for maintenance of proper acid

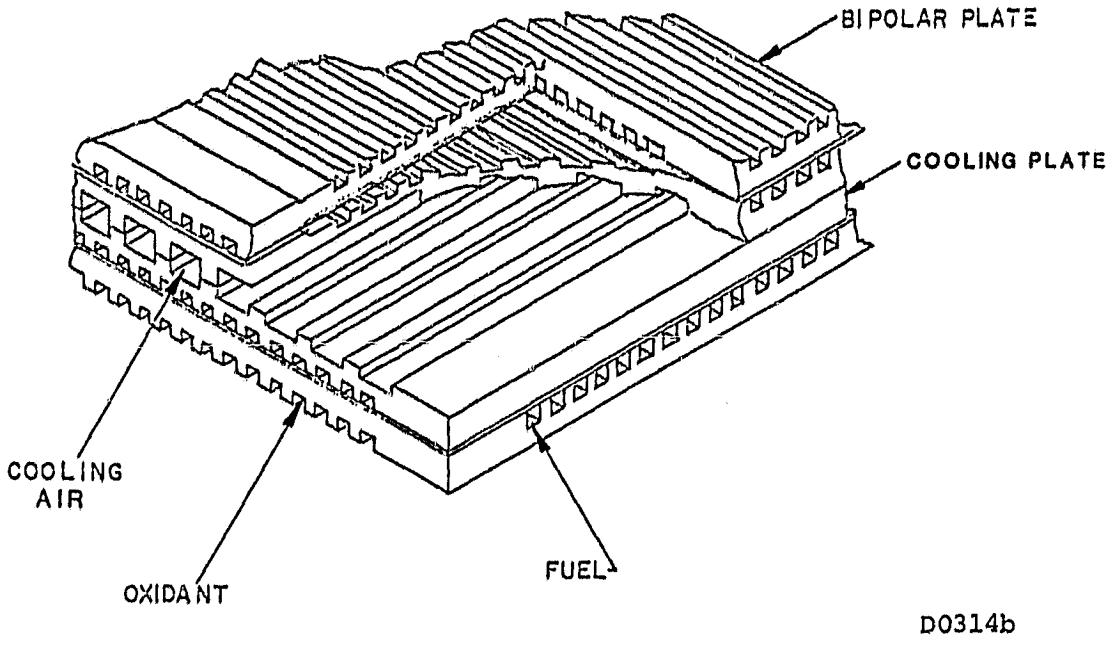

FIGURE 1 PERSPECTIVE VIEW OF A DIGAS STACK

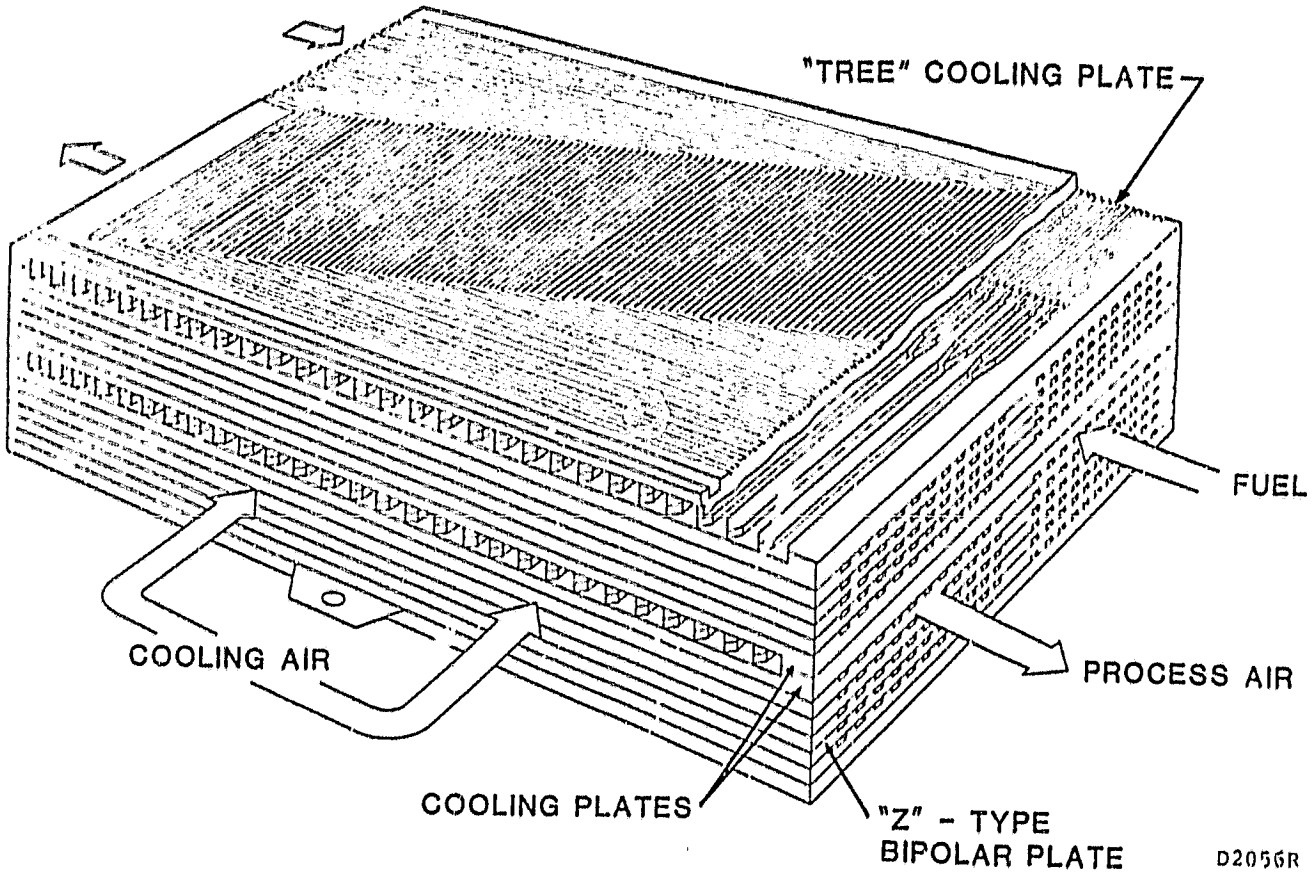

FIGURE 2 PERSPECTIVE VIEW OF THE SEPARATED GAS-COOLED STACK

volume for the pressurized gas cooled PAFC are also discussed. This study provides the proof-of-concept (POC) test data and establishes the feasibility of gas-cooling in pressurized fuel cells.

This report describes the accomplishments of various tasks leading to the testing of the proof-of-concept stack. The initial pressurized testing experience was gained on a facility already constructed under a previous program for 350-cm^2 size cell-stacks (Task 2). In parallel, a more elaborate test facility for 1200-cm^2 size cells was fabricated under Task 1, and short stacks were tested on this facility under Task 3. Design, construction and testing of a 10 kW size proof-of-concept (POC) stack was carried out under Task 4. The analysis of the data obtained on the POC stack was carried out under Task 5. The testing of the 10 kW stack at pressures was performed at Westinghouse's AESD, Pittsburgh facility.

TASK 1. DESIGN AND CONSTRUCTION OF TEST EQUIPMENT FOR 12 x 17 inch (1200-cm^2) STACK TESTING

1.1 OBJECTIVES

The objectives of this task were to design, construct, and check out a test facility with the following features:

- Pressure testing a short 1200-cm^2 fuel cell stack at 100 to 1000 kPa, 50 to 400 mA/cm^2 and 150 to 200°C
- Continuous unattended operation under fail-safe conditions
- Recirculated gas cooling of a pressurized fuel cell
- Automatic data acquisition

1.2 PRESSURIZED TEST STATION DESIGN

A detailed flow diagram of the pressurized test facility showing the control elements is given in Figure 1.1. The pneumatic controllers were selected over the electronic controllers because of the lower system cost. A computerized data acquisition system was also included. Parallel control valves were used in the fuel and oxidant lines to facilitate efficient pressurization and depressurization for most of the expected flows. The features included in the test facility are summarized below:

Flow Configuration

- Countercurrent/cocurrent reactant flow
- Gas cooling of stacks using a separated recirculating scheme

Operation

- 100 to 1000 kPa and 50 to 400 mA/cm^2 testing
- Data scanning and recording by an automatic data acquisition system

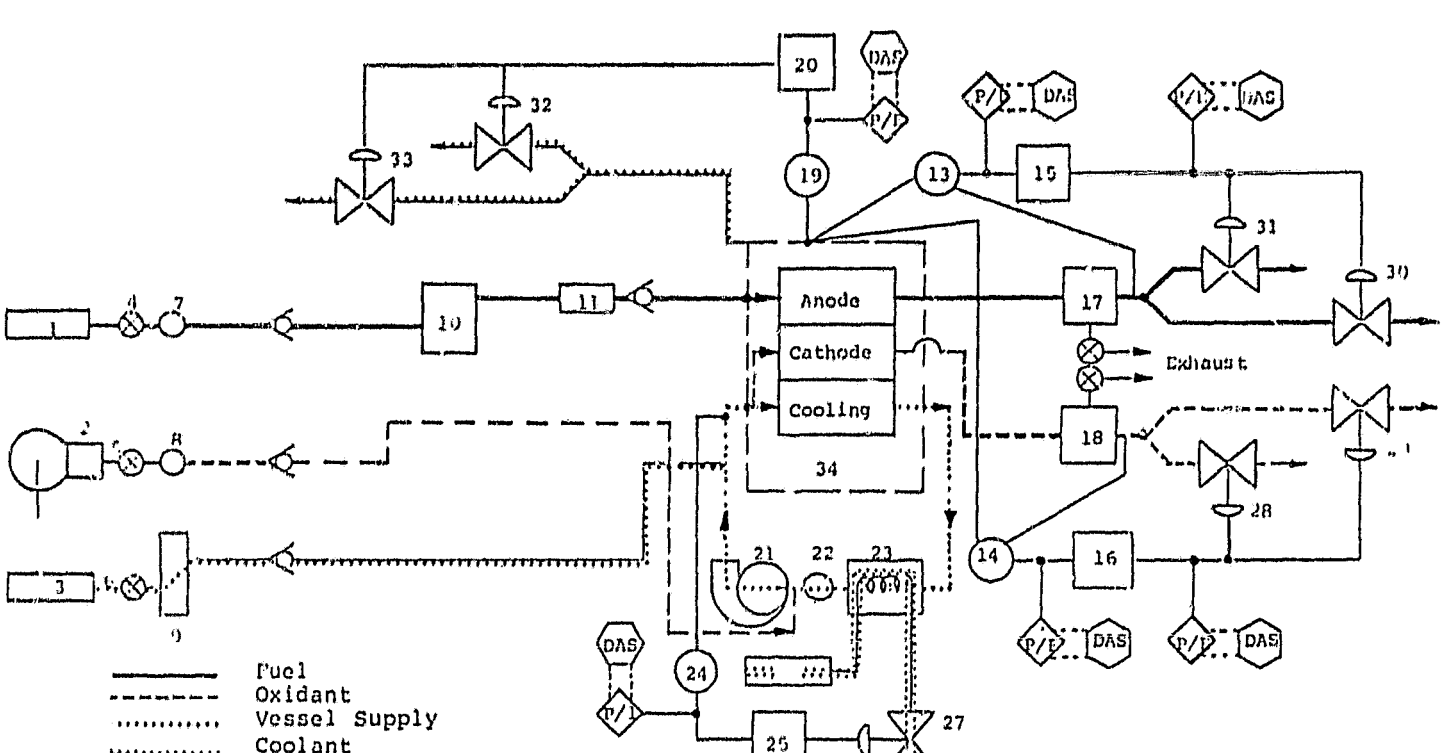

1 Fuel Supply
2 Air Compressor
3 Vessel Atmosphere Supply
4-6 Pressure Regulators
7-8 Mass Flow Controllers
9 Rotameter
10 Vaporizer/Preheater
11-12 Preheaters
13-14 Differential Pressure Transmitters
15-16 Differential Pressure Controllers
17-18 Condensers
19 Pressure Transmitter
20 Pressure Controller
21 Recirculatory Blower
22 Mass Flow Meter
23 Heat Exchanger
24 Temperature Transmitter
25 Temperature/Flow Controller
26 Coolant Supply
27 Coolant Control Valve
28-32 Pressure Control Valves
33 Manual Valve
34 Pressure Vessel

D1108b

FIGURE 1.1 TEST STATION FOR PRESSURE TESTING 12 x 17 in. FUEL CELL STACKS WITH THE RECIRCULATION LOOP

- Unattended round-the-clock pressurized operation
- Reactants simulating actual fuel cell operating compositions

Safety and Stack Protection Features

- Stack overheating protection
- Low cell voltage protection
- Electric power failure protection
- H_2 level monitor in the vessel and room
- CO monitor in room
- Automatic shutdown (maintaining differential pressures of ± 13 cm of water)

Controlled Operating Parameters

- Vessel pressure (pneumatic control)
- Current (manual)
- Hx coolant flow rate (manual)
- Temperatures: air, fuel, cooling and cell (temperature controller)
- Fuel compositions (manual)
- Air and fuel flow rates (manual)
- Recirculated cooling flow (manual)
- Fuel humidity (manual)
- Blower speed (manual)
- Cathode to vessel and anode to vessel differential pressures (pneumatic control)
- Water level in the condenser water trap (automatic)
- Variable pressure drop in the recirculation loop (manual)

Performance Measurements

- Cell Voltage
- Temperature distribution
- Pressure drop across stack in all streams (only one stream per test)

The design details of some of the important subsystem components are discussed below.

- PRESSURE VESSEL: A pressure vessel fitted with a blind flange was designed according to the ASME code to operate at 2200 kPa and 177°C and to test up to 52-cm tall 1200-cm^2 (12 x 17 inch) size fuel cell stacks. The vessel was made of carbon steel; the vessel bottom and the flanges were faced with SS-316.

- PRESSURE FITTINGS: Voltage leads, thermocouple wires and solid conductors penetrating into the pressure vessel from the test panels are to be sealed against the operating pressure of the vessel. Conax type sealant glands are commercially available. An alternate, simpler means for sealing electrical wires, thermocouples and solid conductors was developed and successfully implemented.

- HEAT EXCHANGER: A shell and tube heat exchanger equipped with three baffles was designed and fabricated for removing heat from the fuel cell recirculation loop. In this design hot recirculated gas passes through the shell side, and the cooling air passes through the tube side.

- FUEL HUMIDIFIER: Dry fuel (a mixture of H_2, CO and CO_2) was humidified to simulate the fuel composition obtained from a fuel processor. A positive displacement pump was used in combination with an electrically heated vaporizer.

- BLOWER FOR THE RECIRCULATION OF HOT GASES: A blower is required to force the hot recirculated cooling gases through the stack and the recirculation loop. An axial blower is the preferred type for simplicity of implementation of the recirculated gas cooling concept because it can be located within the flow duct. The standard specifications for commercially

available blowers often rate the operating temperature of the blower motor at less than the operating conditions encountered in the recirculation loop of the gas cooled fuel cell. The life of a blower is a strong function of motor housing temperature and, therefore, indirectly of the bulk gas temperature. A simple scheme was developed that allows the use of these low temperature blowers for recirculating hot gases in the gas-cooled fuel cell system. This scheme is illustrated in Figure 1.2. The available fresh air feed is introduced at the intake of the blower. Then by manipulating the hydrodynamics of this fresh feed, the room temperature air is used as the blower motor envelope to shield the blower motor assembly from the hot bulk gases. The capability of this arrangement for maintaining the blower motor temperature at a much lower point than the bulk gas temperature was first demonstrated. Following this, an axial blower was used in a similar arrangement for circulating the hot gases of the recirculation loop.

- RECIRCULATION LOOP: The recirculation loop is necessary to implement the recirculated gas cooling of the pressurized PAFC stacks. A schematic view of the recirculation loop given in Figure 1.3 shows the location of the different instruments. A mass flowmeter (Thermal Instrument, Model 60) with a DC signal output was used to measure the recirculated gas flow rate in the loop. As discussed earlier, a Rotron Aximax 3 blower (Model 470 JH) was used to circulate the coolant flow. The speed of the blower was varied by a power supply which provided a variable frequency output with tracking voltage. A manual speed control mode was used; however, the computer set speed control mode is available. A butterfly valve was used for manually restricting the recirculation flow to meet blower stability requirements. A flexible pipe piece was introduced to allow for accumulated tolerance error and misalignments that could be caused by an uneven torquing of the flanges, and to accommodate thermal expansion.

- DATA ACQUISITION SYSTEM (DAS): A Kaye Instruments scanner was used for reading the measured variables (current, flow rates, temperatures, voltages, pressure, and differential pressures). An Apple II Plus microcomputer was used for data recording and data manipulation. The system used a floppy disk for data storage.

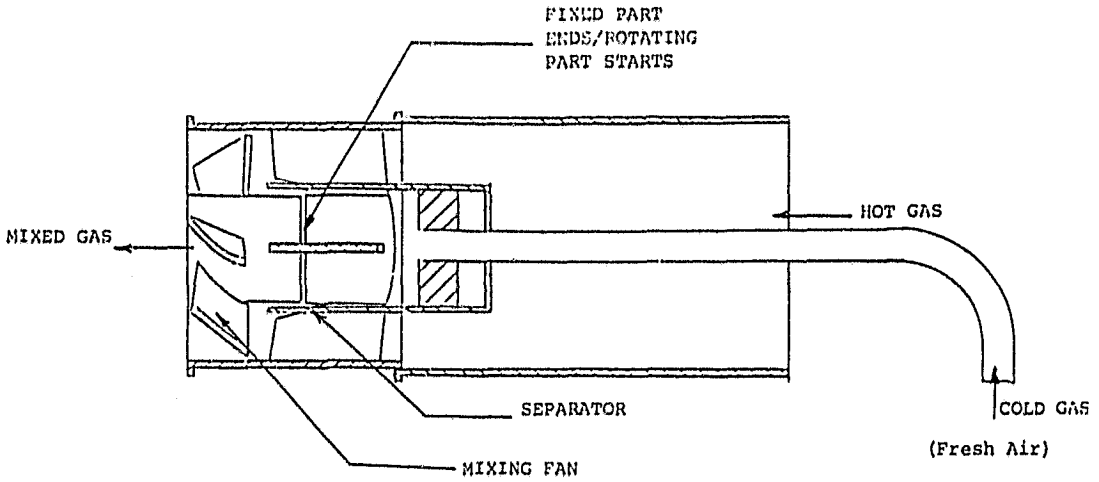

a A CROSS-SECTIONAL SCHEMATIC VIEW

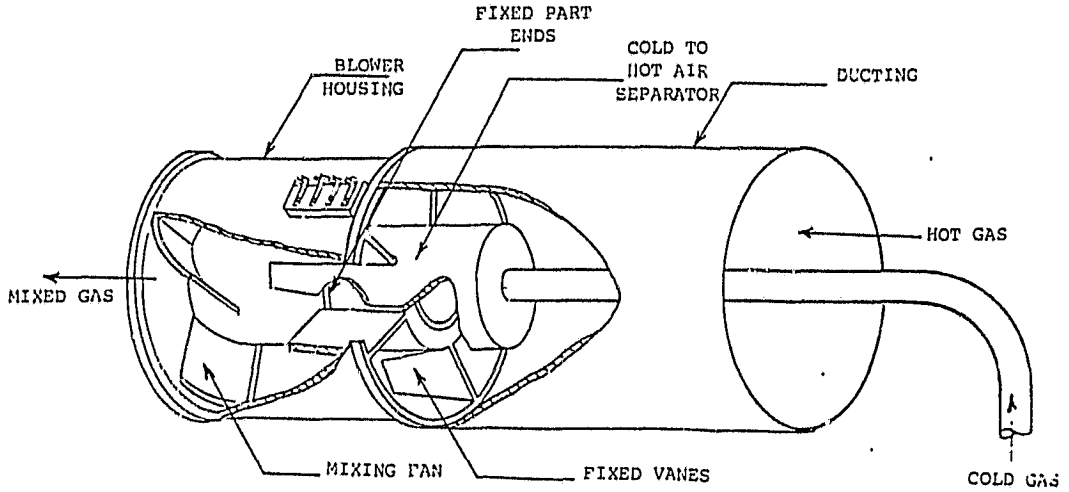

b AN ISOMETRIC REPRESENTATION OF THE ARRANGEMENT

D1471a

FIGURE 1.2 ARRANGEMENT FOR SHIELDING THE BLOWER MOTOR ASSEMBLY FROM THE HOT BULK GASES

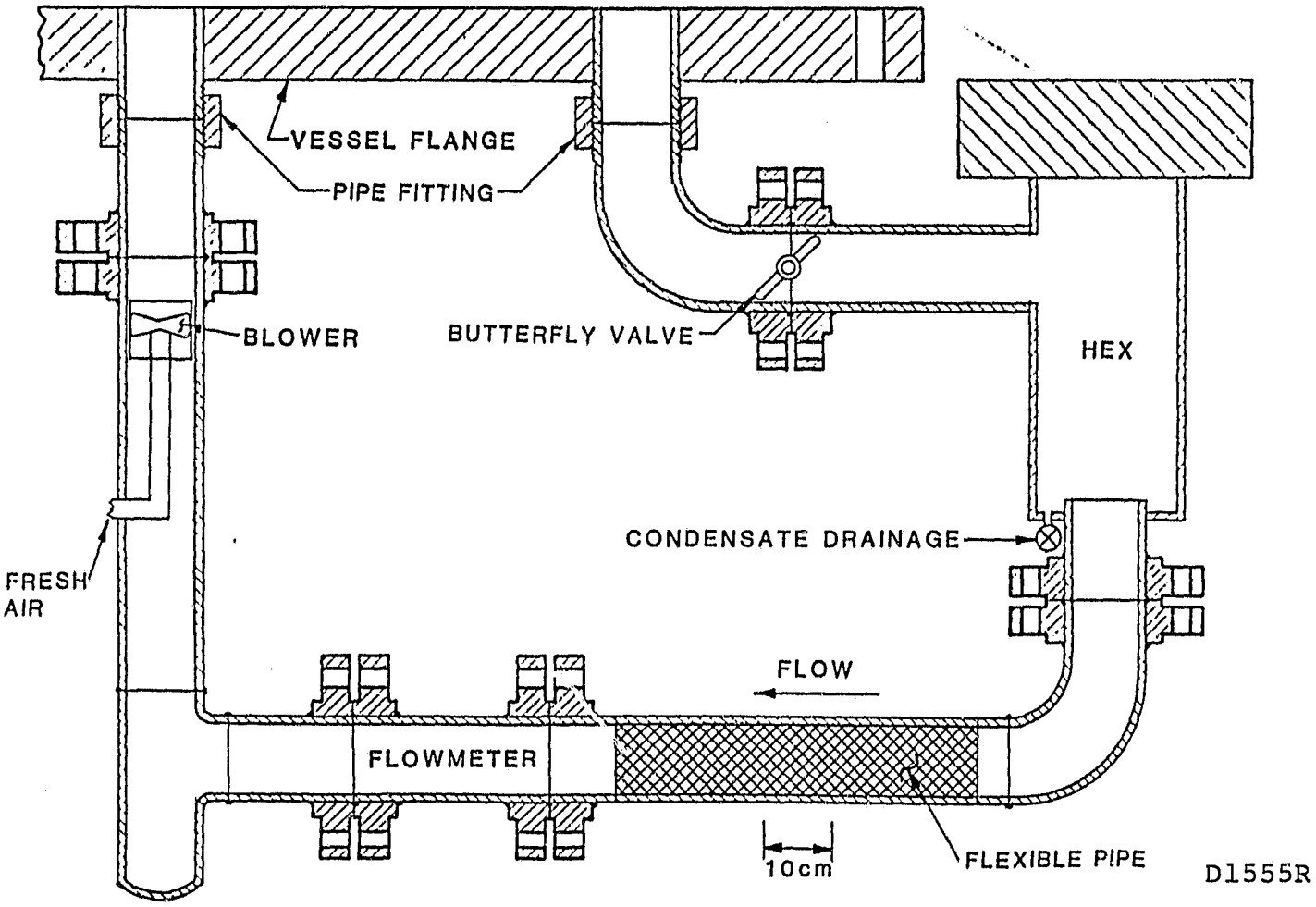

FIGURE 1.3 A SCHEMATIC VIEW OF THE RECIRCULATION LOOP

1.3 TEST FACILITY CONSTRUCTION

A photograph of the completed test station is shown in Figure 1.4. This test station is also capable of operating in a completely manual mode. All the controls are accessible from the test panel. Flexible Nylo-Seal tubing was used for the test station plumbing. The panel was mounted on wheels for mobility and almost all vessel to panel connections used Nylo-Seal tubings and easy to connect fittings. Once the test station construction was completed, check out runs were performed. The complete readiness for pressurized stack testing was demonstrated through successful pressure testing of the Stack P12-1, a 6-cell 1200-cm^2 size stack (separated air-cooled design). The operation of the ERC-built pressure fittings and air cooled axial blower, and the continuous unattended functioning of the test facility under fail-safe conditions were successfully demonstrated.

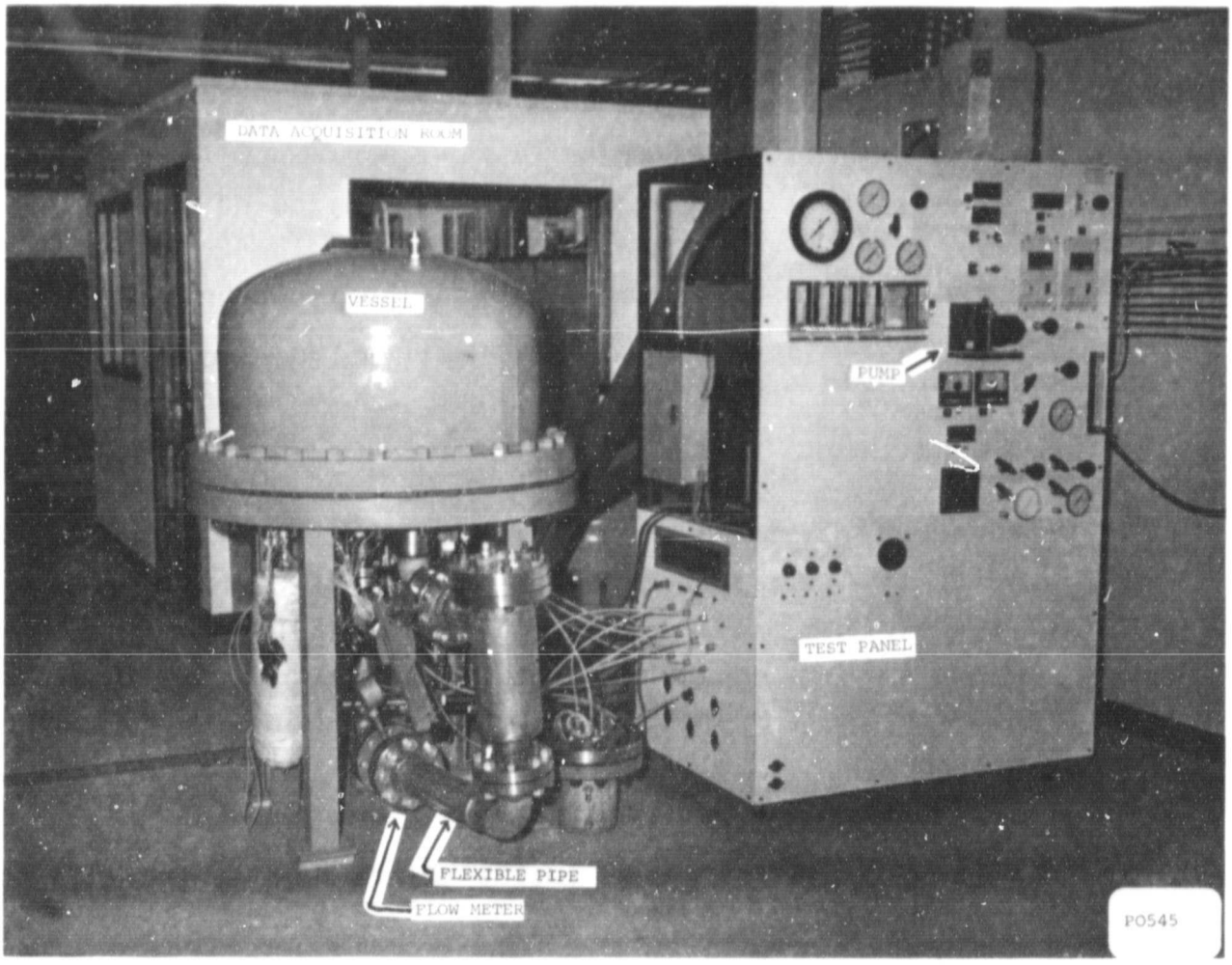

FIGURE 1.4 TEST STATION FOR PRESSURE TESTING 1200-cm^2 SHORT STACKS

TASK 2. TESTING AND EVALUATION OF 350-cm^2 (5 x 15 inch) SHORT STACKS

2.1 OBJECTIVES

The objectives of this task were:

- To gain experience in pressurized testing of gas-cooled stacks
- To study pressurization-depressurization schemes
- To evaluate state-of-the art fuel cell components for pressurized application.

2.2 DESIGN OF STACK COMPONENTS

Three 6-cell, 350-cm^2 (5 x 15 inch) stacks (P5-1, P5-2 and P5-3) were built and tested. Each stack had six cells, having a cooler placed in the middle. Fuel flowed in the short direction while process air and cooling air flowed along the long direction. This design also incorporated the distributed gas (DIGAS) cooling scheme, which involved the splitting of process-and cooling-gas in the same manifold. The cooling plate consisted of two halves, each having molded process channels (anode or cathode) on one side, and a machined straight-through channel (in the 15-inch direction) on the other side. The bipolar and cooling plates were heat-treated to 900°C.

The three cells (Cells 1-3) on one side of the cooling plate were assembled with an acid inventory control member (AICM) developed under Contract DEN3-67 (7) and produced by controlling the amount and distribution of wetproofing in the anode backing. The AICM was used for storing and/or supplying electrolyte as the electrolyte volume in the cell changed during transients. The rest of the cells (Cells 4-6) used a standard anode backing. The acid addition channels for the two groups of cells were isolated to provide separate acid addition capability.

2.3 TESTING OF 350-cm^2 STACKS

The first stack (P5-1) was used for trouble shooting and successful checkout testing of the test station. The later stacks (P5-2 and P5-3) were used in the actual pressure tests. Prior to pressurization, Stacks P5-2 and P5-3 were run at atmospheric conditions for $\sim$1000 and $\sim$500 hours, respectively. Test results are summarized below.

- ATMOSPHERIC PRESSURE PERFORMANCE: The initial performance of all the cells in Stacks P5-2 and P5-3, including the ones with AICMs, were representative of ERC's state-of-the-art stacks. Furthermore, excellent oxygen gains (62 mV @ 33% oxidant utilization) and a performance difference of 6 mV between 15% CO_2/85% H_2 and 100% H_2 indicated that the diffusion polarizations at both anodes and cathodes were negligible in all cells, including the ones with AICMs.
- PRESSURIZED GAIN: The pressurized performance gain of Stacks P5-2 and P5-3 are compared in Table 2.1. The theoretical gain due to pressurization (Nernst and cathode polarization) is:

$$\Delta V = 1.5 \frac{RT}{F} \ell n \frac{P_2}{P_1}$$

$$= 0.085 \text{ V for } P_2 = 450 \text{ kPa (4.4 atm. T; 169°C)}$$

From the experimental results, it can be seen that the observed gain in the terminal voltage was higher than the theoretically predicted gain and, in addition to this, the performance gain was current density dependent. These observations can be explained as follows:

a) Pressurized operation leads to reduced diffusion losses.

b) Pressurization to 445 kPa from atmospheric conditions is expected to change the average acid concentration from 101 to 97%. The higher ionic conductivity of the 97 wt% acid is expected to lower the stack resistance by about 0.2 mΩ. Furthermore, the accompanying acid volume expansion may cause a better wetting of the matrix. Upon pressurization, drops in resistance of 1.0 mΩ and 0.7 mΩ were observed for Stacks P5-2 and P5-3, respectively.

TABLE 2.1 PERFORMANCE GAIN IN PRESSURIZED 350-cm^2 STACKS

(Air Utl.: 50%; Fuel Utl.: 70%; Average Temp.: 169°C)

CURRENT DENSITY, mA/cm^2	STACK P5-2			STACK P5-3		
	PERFORMANCE mV		GAIN, mV	PERFORMANCE mV		GAIN, mV
	101 kPa (1 atm)	445 kPa (4.4 atm)		101 kPa (1 atm)	445 kPa (4.4 atm)	
100	657	750	93	639	733	94
150	617	719	102	605	702	97
200	586	693	107	572	680	108
250	555	665	110	545	657	112
300	509	637	128	518	636	118

- START-UP/SHUTDOWN PROCEDURES: Three different start-up/shutdown approaches were studied using the 6-cell stacks. The main features of these methods are compared in Table 2.2. For the initial pressurization-depressurization runs, a multistep, slow, and very conservative scheme was successfully adapted. (Method 1 was developed in 25-cm^2 cell testing.) Later, a faster, more practicable, one step approach (Method 2) was also successfully employed. This scheme of pressurization-depressurization is accomplished under no-load conditions. Therefore, the differential pressure over-shooting during transients is minimized (because a smaller net flow is involved). In the case of a multi cell stack under no-load conditions, the blower for recirculating the cooling gases need not be operated during pressurization. The blower design therefore becomes much simpler.

  Before pressurization-depressurization starts, the cell temperature is brought down to the desired value by gradually lowering the load. Although the stack is submitted to the open circuit condition, the corrosion rate is comparable to the normal running conditions because a low temperature is maintained during pressurization. The fastest scheme (Method 3) was only tested to study the emergency shutdown approach. The stacks withstood start-up/shutdown procedures of Methods 1 and 2, and the shutdown approach of Method 3, without any observable permanent loss in stack performance.

- EFFECT OF CO_2 AND CO ON PRESSURIZED PERFORMANCE: Stack P5-3 was run on both the pure H_2 and simulated fuel (75% H_2, 24% CO_2 and 1% CO). The pressurized (445 kPa) performance of this stack on these fuels is compared in Figure 2.1. Of the observed 20 mV loss at 150 mA/cm^2, about 11 mV accounts for a CO_2 dilution effect (Nernst loss). The CO_2 and CO related loss in Stack P5-3, at current densities higher than 150 mA/cm^2, appeared to be current density dependent. The stack performance was also studied at three additional pressures (101 kPa, 240 kPa, and 340 kPa). These experiments did not indicate a noticeable effect of the pressure on the CO_2 and CO related performance loss. The CO_2 and CO related loss for the cells with an AICM anode backing was not any different from those with standard backings.

TABLE 2.2 COMPARISON OF START-UP/SHUTDOWN PROCEDURES

FEATURES	METHOD 1	METHOD 2	METHOD 3 (EMERGENCY SHUTDOWN)
Pressurization-Depressurization Rate *	≈ 2 kPa/min	≈10 kPa/min	≈25-75 kPa/min
Current Density	50-100 mA/cm^2	No Load **	No Load
Process Flows	Large	Small	Small
Steps	Multistep	One Step	One Step
Cell Temp.	Normal Cell Temperature	Low Cell Temp. ≈ 150°C	Normal Cell Temperature
Advantages and Disadvantages	Inherently slow because of vapor condensation and transient differential pressure considerations. Requires continuous operation of the recirculation blower.	Corrosion rate is comparable. Blower design will be simpler. Differential pressure control during transient becomes simpler.	This emergency shutdown procedure is the fastest.

*Does not represent the optimum rate.

**Before depressurization/pressurization starts, the cell temperature is brought down to the desired value by gradually lowering the load.

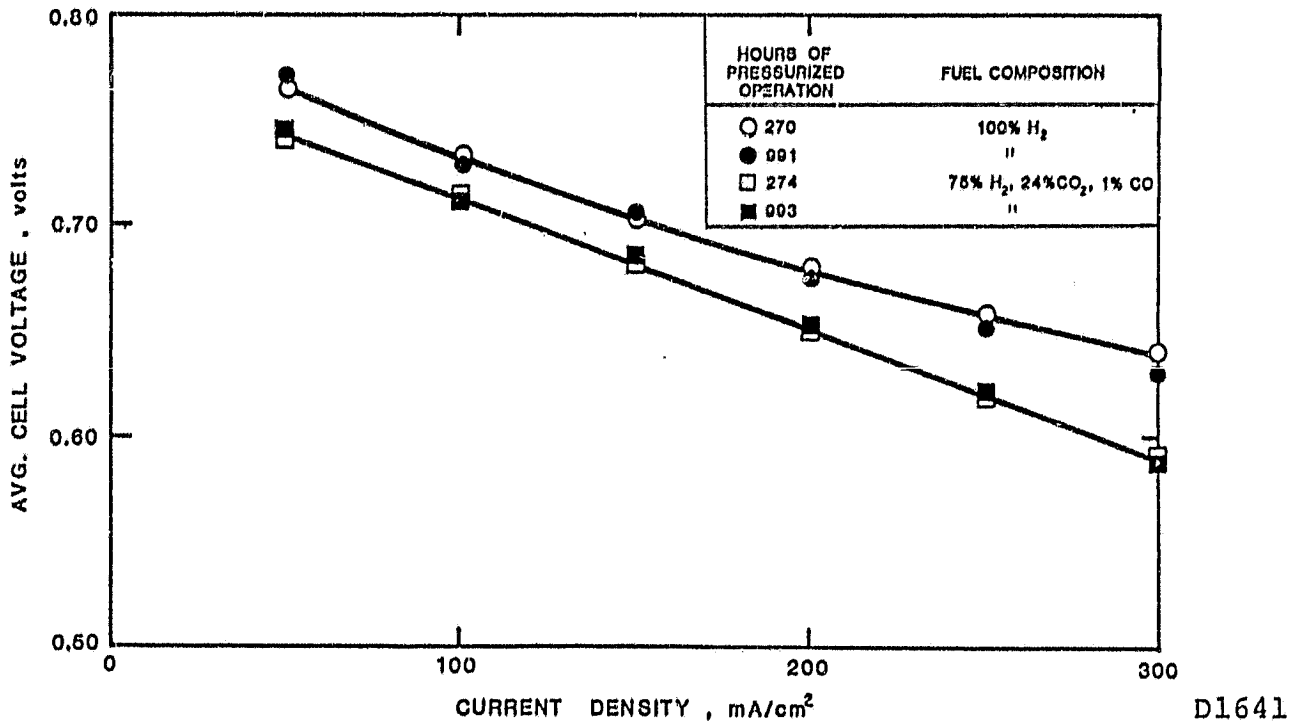

FIGURE 2.1 PRESSURIZED PERFORMANCE WITH DIFFERENT FUELS, STACK P5-3 (Pressure: 445 kPa (4.4 atm.); Fuel Utilization: 70%; Air Utilization: 50%; Average Stack Temp: 169°C)

- EFFECT ON LONG TERM PRESSURIZATION ON PERFORMANCE AND COMPONENTS: Stacks P5-2 and P5-3 were run under pressure for about 1000 hours. In addition, Stack P5-2 had undergone one normal pressurization-depressurization cycle, one emergency shutdown test and 1300 hours of atmospheric testing. Similarly, Stack P5-3 had undergone three normal start-up/shutdown cycles and three emergency shutdown cycles plus an additional 1100 hours of atmospheric testing. The stack performance at all current densities remained stable and the decay in performance during the pressurized study (~1000 hours) was ≤ 3 mV @ 100 mA/cm^2. The pressurized lifegraph of Stack P5-3 (shown in Figure 2.2) also suggests a stable stack performance and resistance throughout.

  Post-test analyses of Stack P5-2 and P5-3 did not suggest any incompatibility of the state-of-the-art atmospheric fuel cell components for a pressurized operation.

- PRESSURE DROP THROUGH PROCESS AND COOLING CHANNELS: The pressure drop in the air flow direction of Stack P5-3 was continously monitored and the results are summarized in Figure 2.3. The experimentally observed pressure drop values were larger than the calculated values. Partial blockage of the process channels by the backing paper (due to sagging) might have caused a reduction in the available flow area, which was probably responsible for the higher observed pressure drops. If a 13% reduction in the process channel depth is assumed, then the experimental pressure drop numbers will exactly match the predicted values. The experimental pressure drop values also confirmed that the pressure drop is inversely proportional to the fuel cell operating pressure. Note that the measured pressure drop values for the flow through the cathode side process channels (at both atmospheric and pressurized operating conditions) remained almost unchanged with time suggesting that no significant reduction of the flow area developed during the testing.

- EVALUATION OF AICM: Test results (Table 2.3) suggest that the use of AICMs resulted in an improved cell performance and the gain in performance was mostly caused by the reduction in cell resistance. In Stack P5-3, the cells using the AICMs recorded about 0.2 mΩ/cell lower resistance as compared with the standard cells. A lower stack resistance due to the use of the AICMs was also observed in other atmospheric stacks. Partial wetproofing of the AICM backing, compared to a total

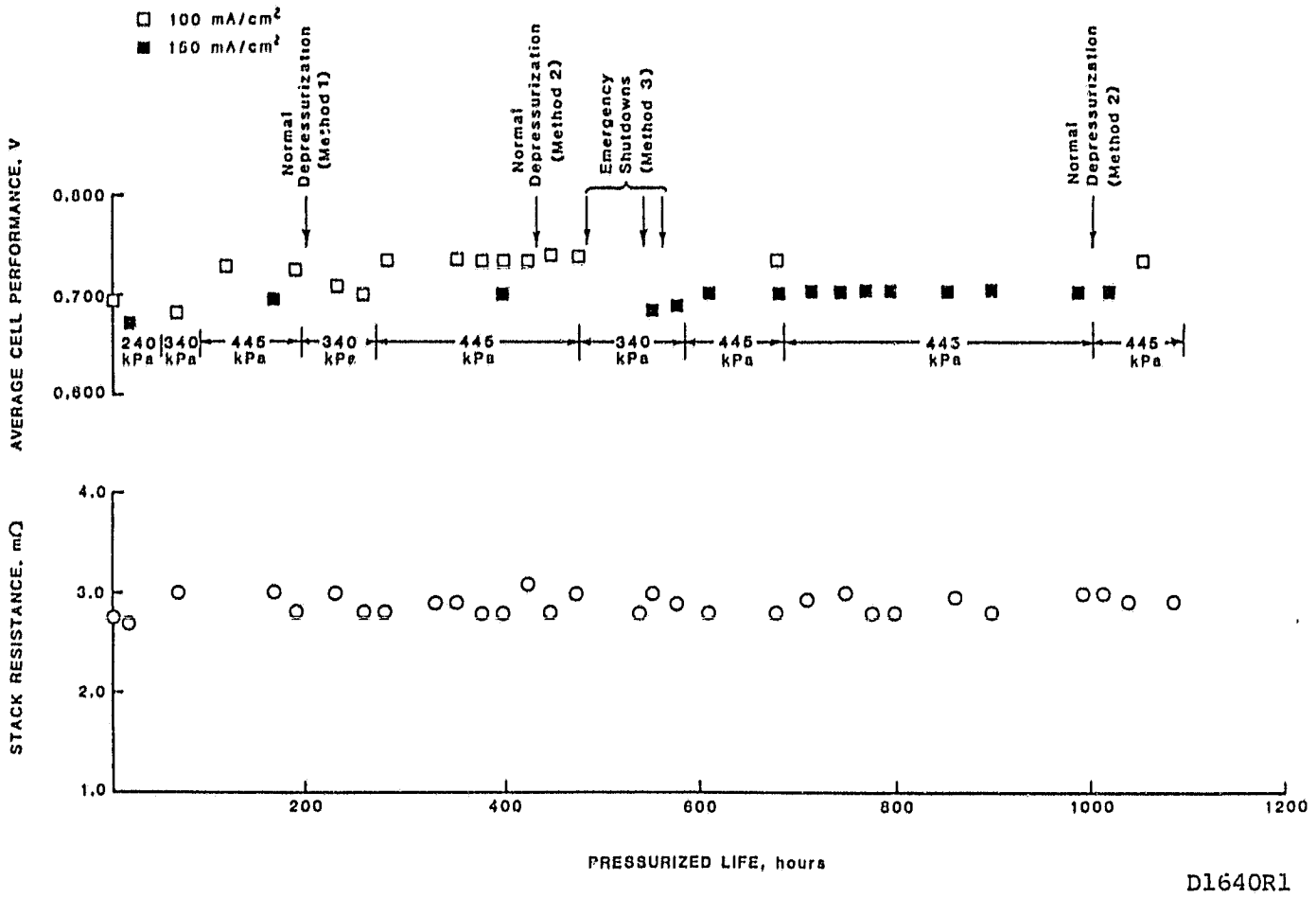

FIGURE 2.2 LIFEGRAPH OF PRESSURIZED STACK P5-3 (Prior to pressurization, the stack was tested under atmospheric conditions for 500 hours)

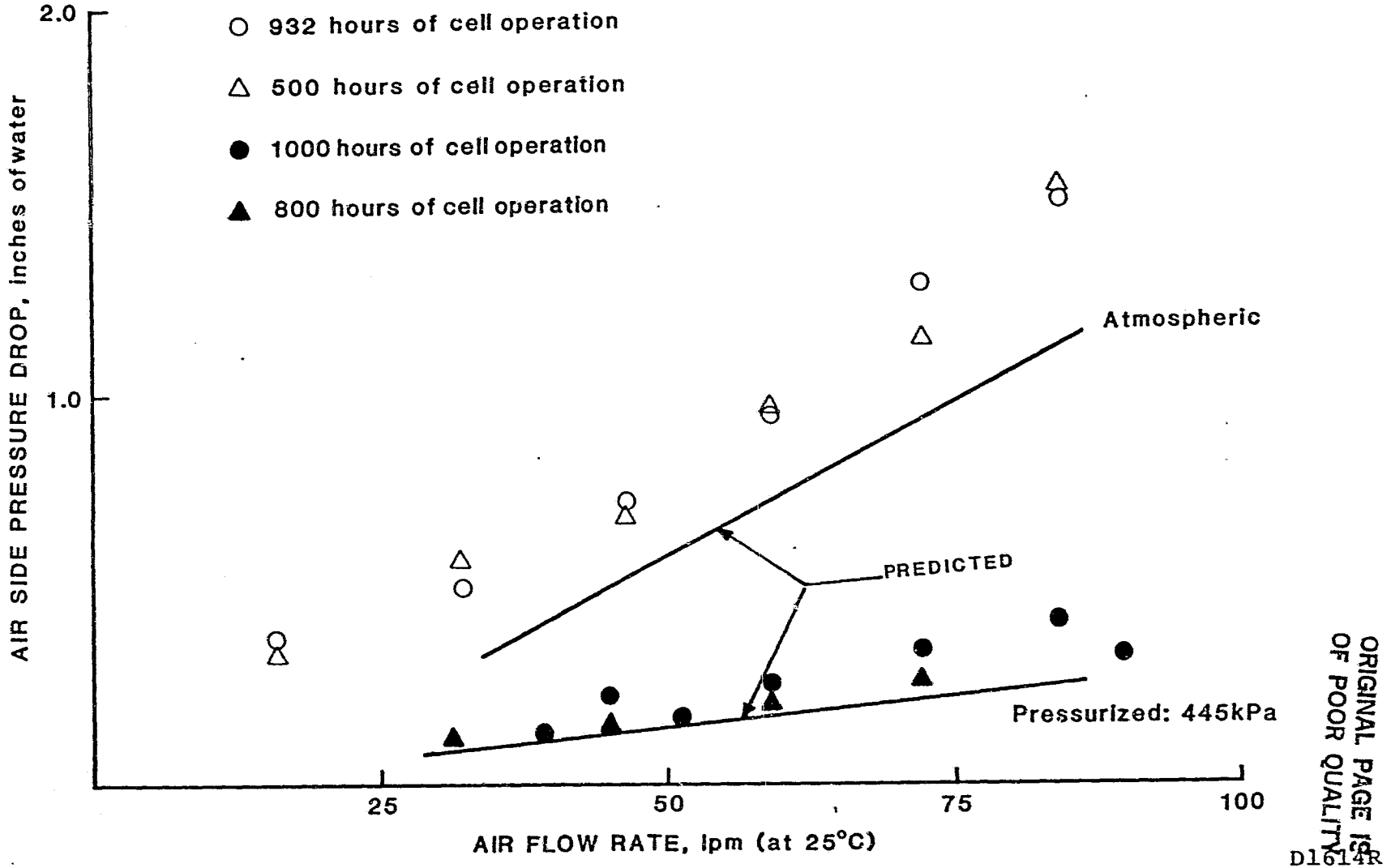

FIGURE 2.3 AIR FLOW RATE Vs PRESSURE DROP, STACK P5-3
(58 lpm correspond to 2 stoich flow through process channel at 150 mA/cm^2; predicted values were calculated using the model of Ref. (6))

TABLE 2.3 NET IMPROVEMENT IN CELL PERFORMANCE DUE TO THE USE OF AICMs

Fuel Utilization: 70%; Air Utilization: 50%; Average Stack Temperature: 169°C; Active Area: 338 cm^2/cell)

STACK	AVERAGE PERFORMANCE @ 300 mA/cm^2, mV			
	ATMOSPHERIC		PRESSURIZED 445 kPa (4.4 atm.)	
	STANDARD BACKING (CELLS 4-5)	AICM BACKING (CELLS 1-3)	STANDARD BACKING (CELLS 4-5)	AICM BACKING (CELLS 1-3)
P5-2	504	522	631	646
P5-3	518 (0.6 mΩ/Cell)	534 (0.39 mΩ/cell)	630 (0.49 mΩ/cell)	654 (0.32 mΩ/cell)

wet-proofing of the standard backing, may have caused the reduction of the contact resistance which is otherwise present at the backing/anode interface.

The stability of the cell resistance in pressurized testing for the cells using the AICMs is shown in Figure 2.4. This suggests an effective acid volume management during acid volume expansion. Pressurization to 445 kPa led to a decrease in cell resistance because of an increase in acid conductivity caused by acid dilution. After depressurization, the cells using the standard anode backing always registered a significant increase in the cell resistance. Both the terminal performance and the IR-free terminal performance recorded a sharp drop, indicating acid starvation symptoms.

In all instances, the acid addition helped to regain both the terminal and IR-free terminal performance, and to lower the cell resistance to the original value (prior to the pressurization). This apparent loss of acid from Cells 4 to 6 is most probably related to the acid volume expansion caused during pressurization. Due to the pressurization to 445 kPa, the acid volume expands (calculated to be about 8% at Stack P5-3's running conditions) and the excess amount is forced out.

The leakage paths appear to be:

1) In-plane through the edge seal into the manifold, most likely into the fuel exit manifold, which is located at the lowest gravity point.

2) Thru-plane across the backing into the process channels.

In Cells 1 to 3, the excess volume of acid can be accommodated inside the nonwet-proofed areas of the AICM backing paper and released to the electrodes when the stack is depressurized and acid volume contraction takes place. These assumptions were supported by follow-up experiments.

After 1960 hours of operation (atmospheric and pressurized) the stack was depressurized from 445 kPa to 101 kPa. As usual, only Cells 4 to 6 registered a resistance increase (from 0.51 to 1.1 mΩ) and suffered a performance loss. The stack was then repressurized to the original pressure (445 kPa) without adding any acid. The original stack resistance and the

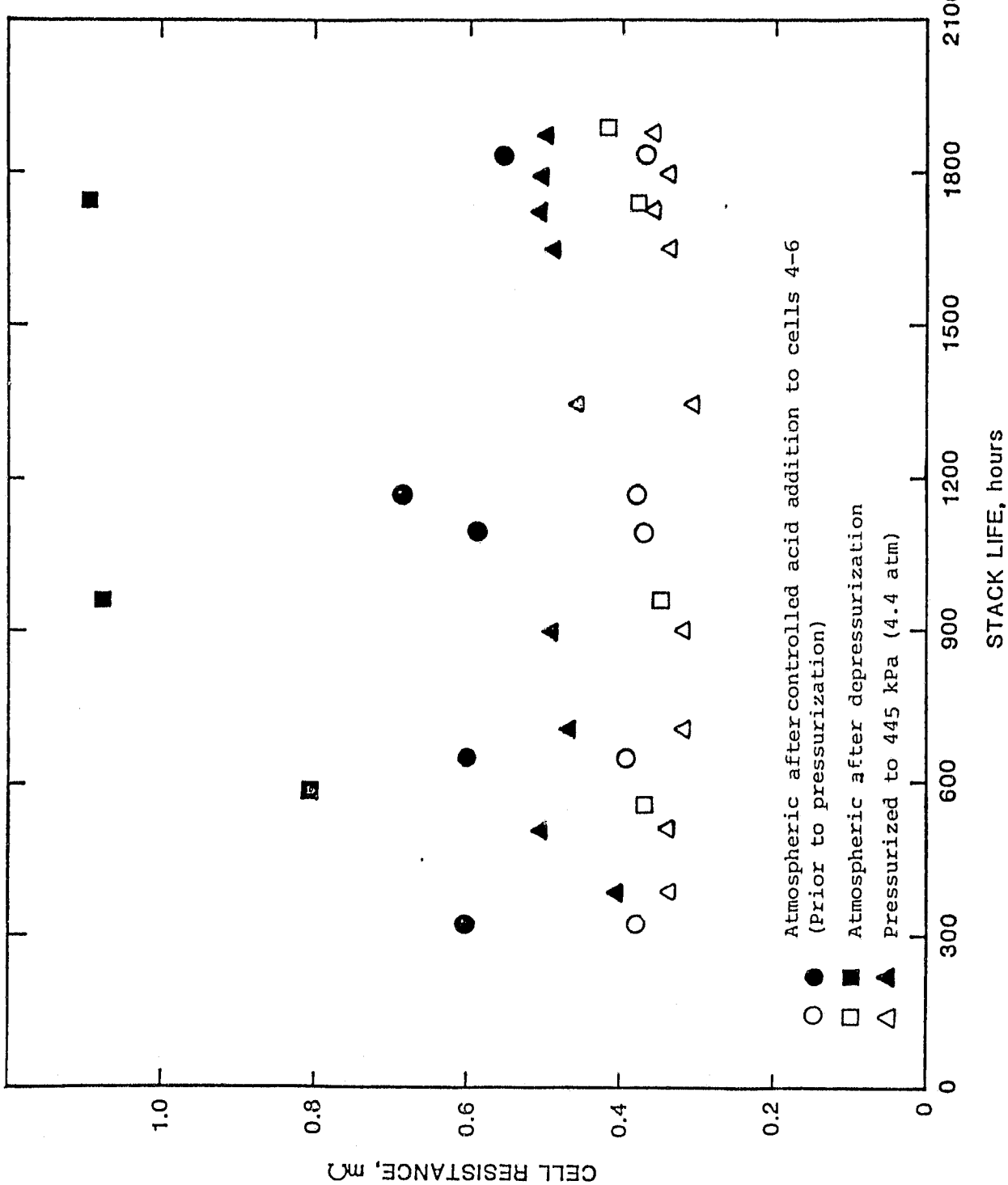

FIGURE 2.4 EFFECT OF PRESSURIZATION & ACID ADDITION ON STACK RESISTANCE (Average Stack Temperature: 169°C; Open Points: Cells with AICM; Filled Points: Cells with Standard Backing)

performance were regained. Next the stack was depressurized and only the acid channels of these cells were completely filled with acid. The stack was then repressurized to 445 kPa. Cells 4 to 6 were observed to be air sensitive. Next the stack was depressurized and disassembled immediately. Acid was observed in the fuel exit manifold. Acid was also found in both the air and fuel flow channels of Cells 4 to 6, blocking about 20-60% of the flow area.

The results discussed so far indicate that the AICM anode backing helped to reduce the cell resistance. In addition, the AICM is also effective in controlling the acid volume change that may occur due to a change in operating conditions or during the transients. Hence, for the stable operations of the pressurized fuel cells, the use of AICMs may be recommended. This would be of even greater importance if pressure variations are used as a means of load management in utility powerplants.

2.4 SUMMARY OF 350-cm^2 SHORT STACKS

Successful pressure testing of the 6-cell 350-cm^2 stacks indicated that:

- Pressure gains higher than the theoretical are obtained for the high current density operation.
- Performance decay during 1000 hours of operation is negligible and state-of-the-art atmospheric components appear acceptable for a short-term pressurized operation.
- Easy to implement and relatively simple start-up procedures do not affect fuel cell performance.
- Acid volume management in pressurized testing is critical and the use of AICMs is recommended to accommodate the acid volume variation and reduce cell resistance.

TASK 3. PERFORMANCE TESTING OF RECIRCULATED GAS-COOLED 1200-cm^2 (12 x 17 inch) SHORT STACKS

3.1 OBJECTIVES

This task was intended for design confirmation testing of separated gas-cooled (SGC) pressurized stacks. Short 1200-cm^2 stacks (6- and 12-cell) were tested to study the following:

- Pressurization and depressurization technique
- Acid volume management procedure
- Baseline performance (cell voltage on pure H_2 & SRF, performance gain under pressure, reactant utilization, component compatability, seal effectiveness, etc.).

3.2 STACK DEVELOPMENT TESTS

The concept of the separated gas-cooling of the fuel cell and the pertinent embodiment was tested for atmospheric use under NASA/DOE Contract DEN3-161 (5, 6). Stacks incorporating a similar design (design details will be discussed under Task 4), were employed in the pressurized stack development testing. Four 6-cell stacks and one 12-cell stack were tested at pressures up to 1010 kPa (10 atm). A summary of these tests is reported in Table 3.1. The results are discussed below.

- START-UP, NORMAL SHUTDOWN AND EMERGENCY SHUTDOWN TESTS: The start-up, normal shutdown and emergency shutdown procedures (discussed under Task 2) were successfully implemented during 101 to 1010 kPa testing of 1200-cm^2 stacks. The pressurization/depressurization rate of 20 kPa/min and the emergency depressurization rate of 101 kPa/min were routinely used while maintaining ΔP fluctuations below $\pm$ 6 cm of water.
- ACID VOLUME MANAGEMENT CONSIDERATIONS: Proper electrolyte volume management is important for maintaining the performance level of a phosphoric acid fuel cell operating at different conditions. Equilibrium electrolyte concentration is a function of the operating variables: temperature, stoichiometric flow of the reactants, inlet gas compositions, and, most importantly, the

TABLE 3.1 STACK DEVELOPMENT TEST SUMMARY

STACK NUMBER	BUILD VARIABLES			ASSEMBLY VARIABLES *					OPERATION				TESTS PERFORMED	REMARKS
	NO. OF CELLS	NO. OF COOLERS	ELECTRODE SINTERING TEMP. °C	ACID ADDED DURING ASSEMBLY		DESRD. COMPRESSION		STACK COMPRESSION	PRESSURE DURATION		ADDITIONAL CYCLES			
				CONC. WT %	QUANT. ml	ANODE mils	CATHODE mils	kPa	kPa	hrs	Pres.-Depres.	Acid Addition		
P12-1	6	1	350	101	43	4-6	4-6	445	101 505 1010	50 3 1	0	0	Checkout of the newly constructed test facility	Defects in the facility were identified and corrected
P12-2	6	1	350	101	43	4-6	4-6	445	101 505 1010	200 50	0	0	Edge-seal optimum acid volume requirement (OAVR), pressurized gain	This stack was later used to checkout another 6-cell 1200-cm² pressurized test facility
P12-4	6	1	350	101	43	1-3	1-3	445	101 505 1010	270 40 15	2	1	Edge-seal, OAVR, pressurization & emergency shutdown, performance on fuel, utilization and pressure drop through cathode process channel	During emergency shutdown ΔP increased over at least 25 cm of water and cells 3 and 4 developed cross-leak
P12-3	12	2	350	101	43	1-3	1-3	445	101 505 1010	620 61 12	1	1	Thermal profile	Low acid content caused difficulties in atmospheric testing.
P12-5	6	1	360	97	50	1-3	1-3	445	101 505	350 130	1	1	OAVR, fuel humidity and short-term continuous pressurized performance	Results suggest that sustained ΔP fluctuations of >10cm of water over long period be avoided for pressurized stacks

*Machined 'Z' and 'tree' patterns on bipolar and cooler plates, respectively, and heat treated to 900°C; 0.3 mg/cm² and 0.5 mg/cm² Pt loading on anodes and cathode, respectively.

operating pressure. Therefore, a change in the fuel cell operating conditions may change the equilibrium concentration, causing an increase or decrease of the acid volume. The changes in the fuel cell acid concentration (Figure 3.1) and acid volume (Figure 3.2) were estimated using the acid vapor pressure data available in the literature (8), extrapolated values of the acid vapor pressure data and simplifying assumptions. Changing the operating pressure from 101 to 1010 kPa at 180°C will decrease the average acid concentration from 100.6 to 91.7 wt% and the associated increase in volume is ~17%. This analysis also indicated that the effects of operating temperature and stoichiometric air flow on the acid volume change becomes more pronounced as the operating pressure increases.

An uncontrolled increase in the acid volume may result in an irreversible loss of electrolyte. Simililarly, an excessive decrease in the acid volume may cause a higher cell resistance and/or reactant cross-leak across the matrix. To override the effects of the acid volume variations, the use of an acid inventory control member (AICM) seemed to be very useful. However, the AICM was not available for use in these developmental stacks. Therefore, to alleviate the effects of an acid volume change, conservative test procedures for start-up/shut-down, pressure and power level changes, etc. were established. All test procedures were designed based on the acid volume variation information (Figure 3.2), experimental considerations and on the assumption that the low acid volume may be less harmful than the excess acid volume. Furthermore, acid added to the stack during the assembly was restricted in order to permit acceptable testing of stacks at pressures between 101 to 1010 kPa.

- BASELINE PERFORMANCE OF 1200-cm^2 STACKS: The cell performances on pure H_2 and simulated reformer fuel (SRF), performance gain at pressure, effect of reactant utilization and pressure vessel temperature, compatability of the state-of-the art component for pressurized operation, etc. were studied using Stack P12-2 through Stack P12-5. The findings are discussed below.

The average cell performances on pure H_2 and SRF (75% H_2, 24% CO_2, and 1% CO on a dry basis) at two different pressures are compared in Figure 3.3. The average performance at 1010 kPa (300 mA/cm^2 and 190°C) was 680mV. The results show that the CO_2-CO related loss at 1010 kPa and 300 mA/cm^2 was 25 mV, and slightly current density dependent at the higher current densities.

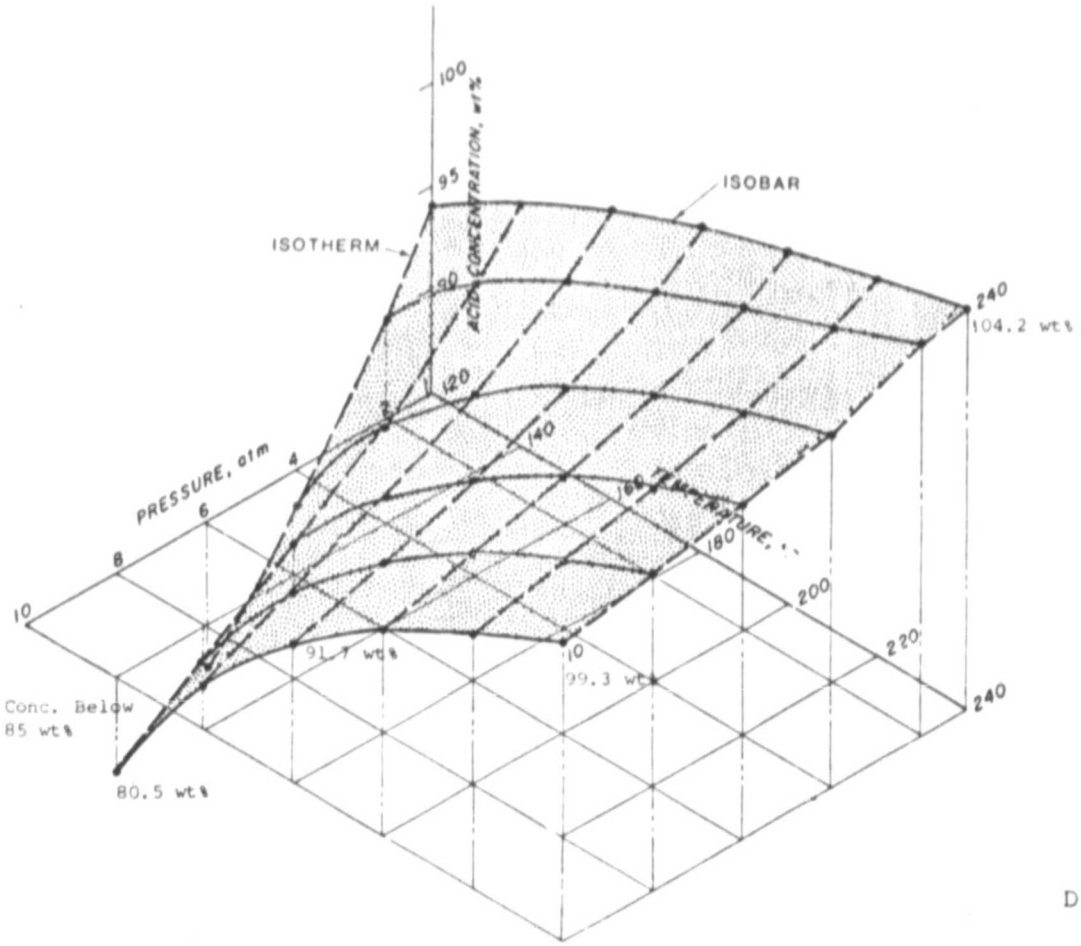

FIGURE 3.1 AVERAGE ACID CONCENTRATION IN A PAFC AS A FUNCTION OF PRESSURE AND TEMPERATURE (Conditions and assumptions are listed below; numerical data is reported in Appendix A)

Conditions:

Mole Fraction of H_2 in Fuel Inlet	0.75	
Mole Fraction of O_2 in Oxidant Inlet	0.208	
H_2 Utilization	80	%
O_2 Utilization	50	%
Partial Pressure of H_2O in Fuel Inlet	53	mm of Hg
Partial Pressure of H_2O in Oxidant Inlet	2	mm of Hg

Assumptions and Approximations:

- All the water produced leaves with the exit gas streams
- Both exit gas streams have the same water partial pressure
- Average acid concentration is in equilibrium with the average water partial pressure

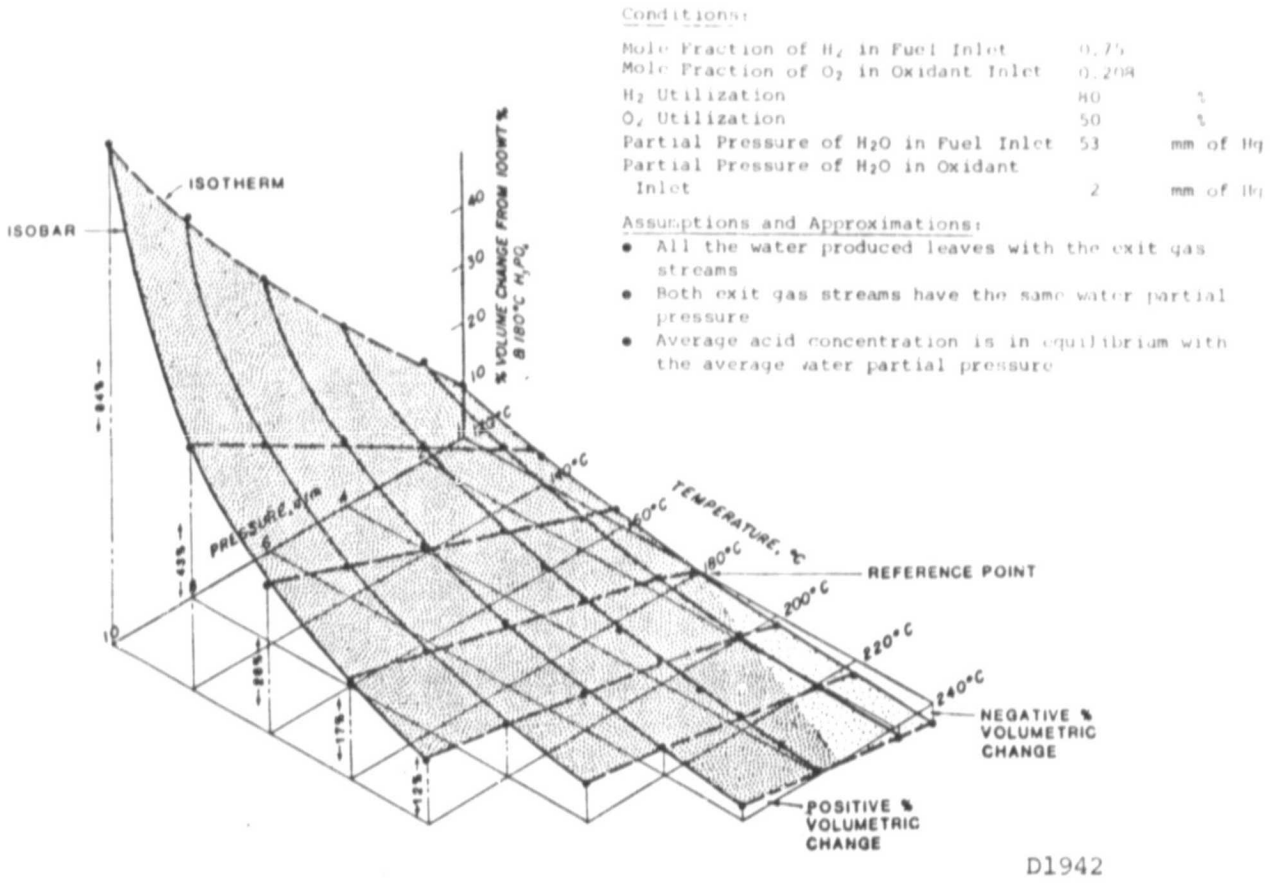

FIGURE 3.2 THE ACID VOLUME CHANGES IN A PHOSPHORIC ACID FUEL CELL (Conditions and assumptions are mentioned above; numerical data is reported in Appendix A)

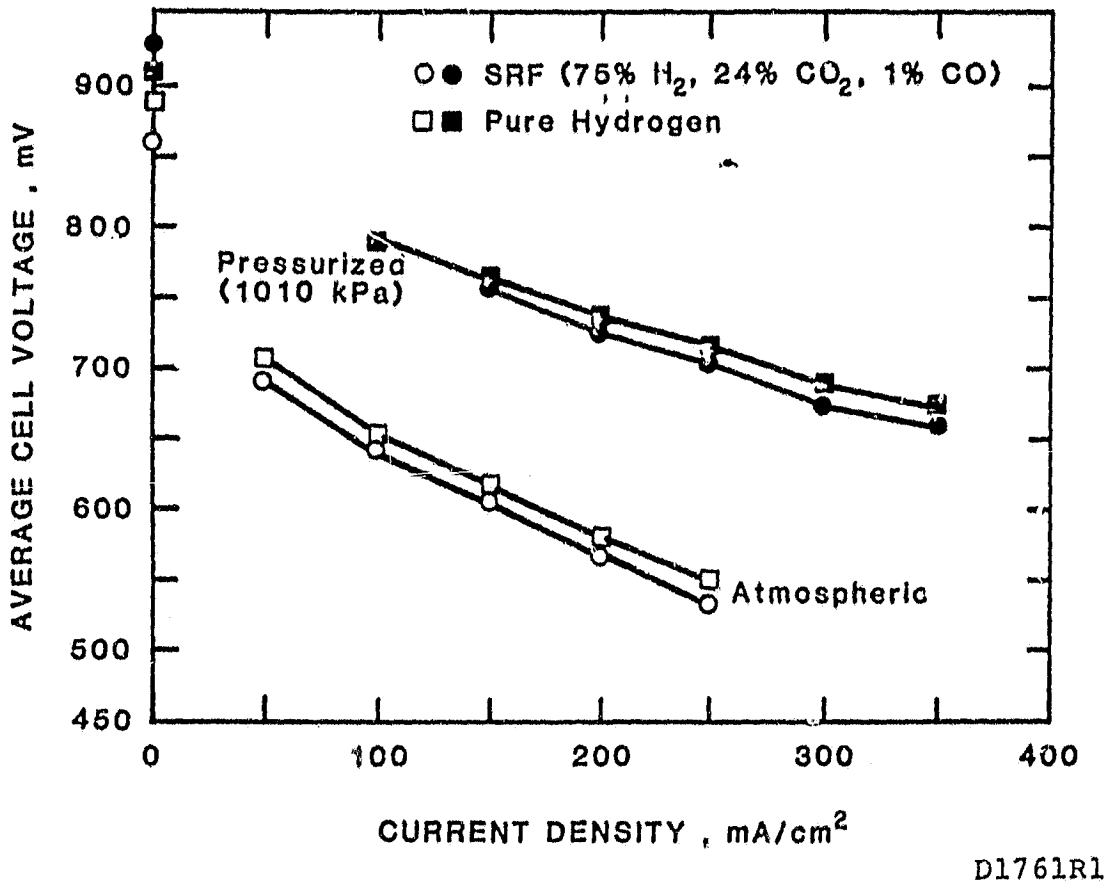

FIGURE 3.3 PRESSURIZED AND ATMOSPHERIC PERFORMANCE, STACK P12-4 (Air Util.: 33%; Fuel Util.: 80%; Maximum Stack Temperature: 190°C; Stack Resistance: 1.50 mΩ)

Typical pressurized gains of individual cells at two different current densities are reported in Table 3.2. The average gain in performance at 150 mA/cm^2 due to pressurization to 505 kPa was 111 mV (theoretical gain is 94 mV), and from 505 to 1010 kPa it was 39 mV (theoretical gain is 41 mV). Note from the results that the gain due to pressurization was different from that predicted and appears to current density dependent.

The effect of fuel (pure H_2 and SRF) and air utilizations on stack performance was studied at different pressures. The performance was insensitive to H_2 utilization for values below 85% (for both pure H_2 and SRF); operating pressure did not make a significant difference to the utilization related performance loss. Note that the cell performance was sensitive to air utilization values higher than 60%.

The effect of fuel humidity on pressurized fuel cell performance was investigated and was found to be almost negligible at all current densities (Figure 3.4). However, contrary to the understanding of the effect of average water partial pressure on fuel cell performance, a slight improvement in the fuel cell performance was observed because of the fuel stream humidification. This probably resulted from a reduction in internal resistance (ionic resistance) of the gas diffusion electrodes and the matrix.

All state-of-the-art fuel cell components were found to be suitable for the short term pressurized testing. However, corrosion of the bipolar plate was noticed in some of the pressurized fuel cells.

The Mat-1 matrix and Teflon shims were employed for the edge sealing of the separated gas-cooled fuel cell stacks. The cell edge seal design (anode and cathode compression of 3 to 5 mils and 1 to 3 mils respectively, a total stack compression of 445 kPa, and a uniform wetting of the Mat-1 matrix sealing edges during the stack assembly) provided an edge seal tolerance to short-term ΔPs of 25 cm of water, and to long-term ΔPs of 10 cm of water.

The gas temperature in the pressure vessel was monitored as a function of the operating pressure. The heat transfer coefficient increases with pressure causing increased heat loss from the fuel cell stack. Therefore, as expected, the temperature in the vessel increased with pressure. The working design temperature for the vessel was 177°C and the vessel temperature stayed below 65°C at 1010 kPa (10 atm).

TABLE 3.2 PERFORMANCE OF INDIVIDUAL CELLS ON PURE H_2, STACK P12-4 (SRF: 75% H_2, 24% CO_2, 1% CO; Maximum Stack Temperature: 190°C; Air Utl.: 33%; Fuel Utl.: 80%)

Cells	PERFORMANCE AND PRESSURE GAINS, mV							
	1 atm	505 kPa (5 atm)			1010 kPa (10 atm)			
	150 mA/cm^2	150 mA/cm^2	Gain at 150 mA/cm^2	300 mA/cm^2	150 mA/cm^2	*Gain at 150 mA/cm^2	300 mA/cm^2	*Gain at 300 mA/cm^2
1	603	724	121	633	769	45	712	79
2	613	728	115	643	815	87	720	77
3	620	725	105	623	750	25	672	49
4	626	726	100	636	729	3	671	35
5	621	731	110	649	769	38	720	71
6	626	737	111	664	777	40	715	51
Avg.	618	729	111	641	768	39	702	61
SRF (Avg.)	609			620			678	

Theoretical gain from 1 to 5 atm is 94 mV and 5 to 10 atm is 41 mV.

*Represents the observed gain from 5 to 10 atm operation.

Prior to 1010 kPa operation, Cells 3 and 4 developed a cross-leak resulting from ΔP excursion during emergency shutdown procedure testing.

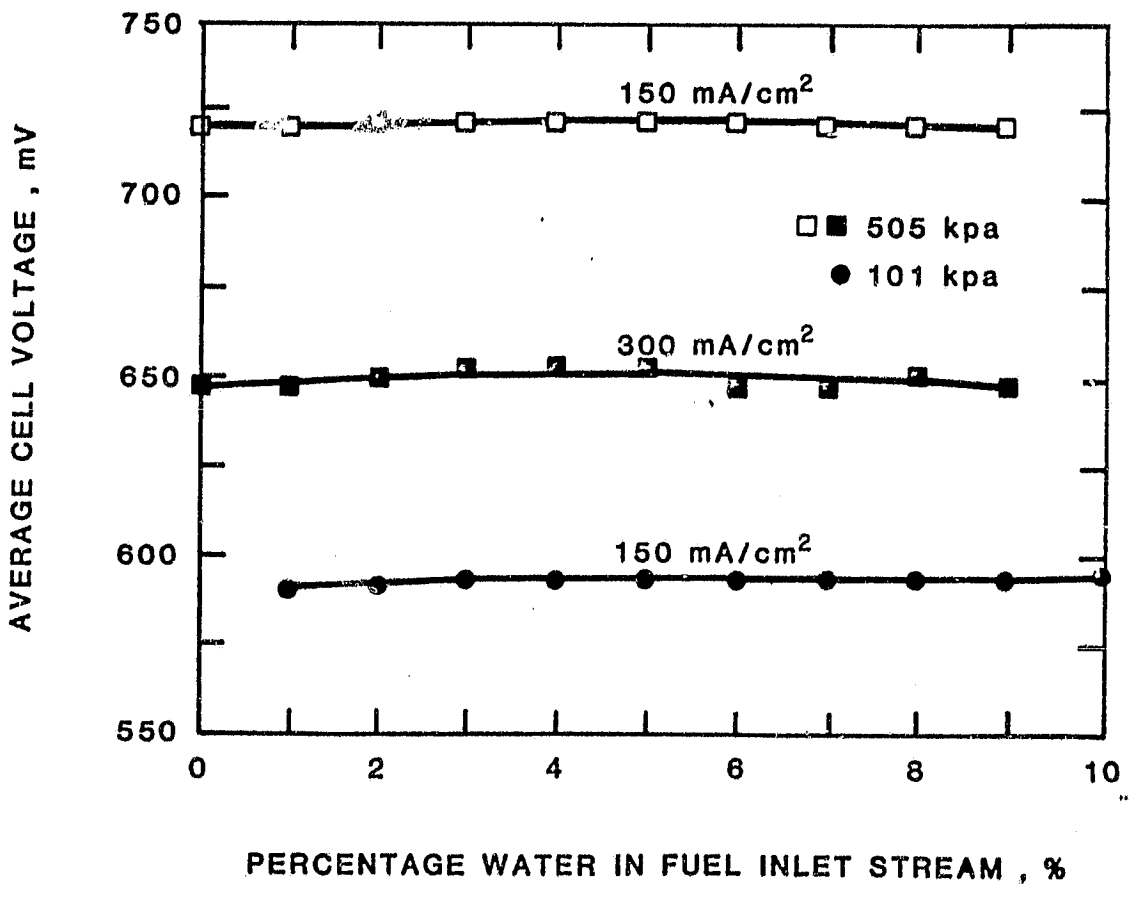

FIGURE 3.4 EFFECT OF WATER CONTENT OF THE FUEL STREAM ON FUEL CELL PERFORMANCE, STACK P12-5 (Air Utl.: 33%; H_2 Utl.: 80%; Max. Stack Temperature: 190°C)

Temperature distribution test data obtained from the 6-and 12-cell stack testing indicated the center cell in a thermal unit (a group of cells having a full cooler at each end) to be the hottest. The observed temperature gradient in a thermal unit in the stacking direction was roughly symmetrical around the center cell and the temperature difference between adjacent cells was approximately 2°C. The cell temperature profile in the reactant and cooling flow directions was reasonably uniform.

3.3 SUMMARY OF PRESSURE TESTING SGC STACKS

The implementation of the separated gas-cooling concept for the pressurized fuel cell stacks was verified through testing of short stacks (four 6-cell stacks and one 12-cell stack). The suitability of the stack design for pressurized testing was also verified.

TASK 4. DESIGN, TESTING AND EVALUATION OF A GAS-COOLED (12 x 17 inch) 10 kW SIZE FUEL CELL STACK

4.1 OBJECTIVES

The objectives of this task were as follows:

- Design cooling plates for gas cooled fuel cell stacks for pressurized operation
- Design and build a 10 kW size gas-cooled fuel cell stack
- Test the 10 kW stack at pressures up to 690 kPa (6.8 atm) to study the effect of operating variables on thermal and electrochemical performance.

4.2 COOLING PLATE DESIGN

The cooling plate design for the pressurized fuel cell utilized analytical models and results developed in a previous program for atmospheric pressure stacks (NASA Contract DEN3-161) (6). Variables considered for this design study include the DIGAS and separated cooling options, 'straight through' and 'tree' cooling channel configurations, and the cooling plate located at an interval of every 3 to 5 cells. Both the 'straight through' and 'tree' designs used channels of a rectangular cross section. In the case of the 'tree' design, the channels progressively branch into additional channels as shown in Figure 4.1. The design allows an increased intensity of local cooling along the path to compensate for an increasing coolant temperature. Details of various 'tree' cooling channel geometries are given in Figure 4.1.

Six different designs were compared on the basis of a pressure drop related auxiliary power loss, the difference between the average and maximum cell temperatures (measure of temperature uniformity) and the net cell voltage. The terminal voltage of a fuel cell increases at a fixed current density due to an increase in cell temperature. It is desirable to maintain the average

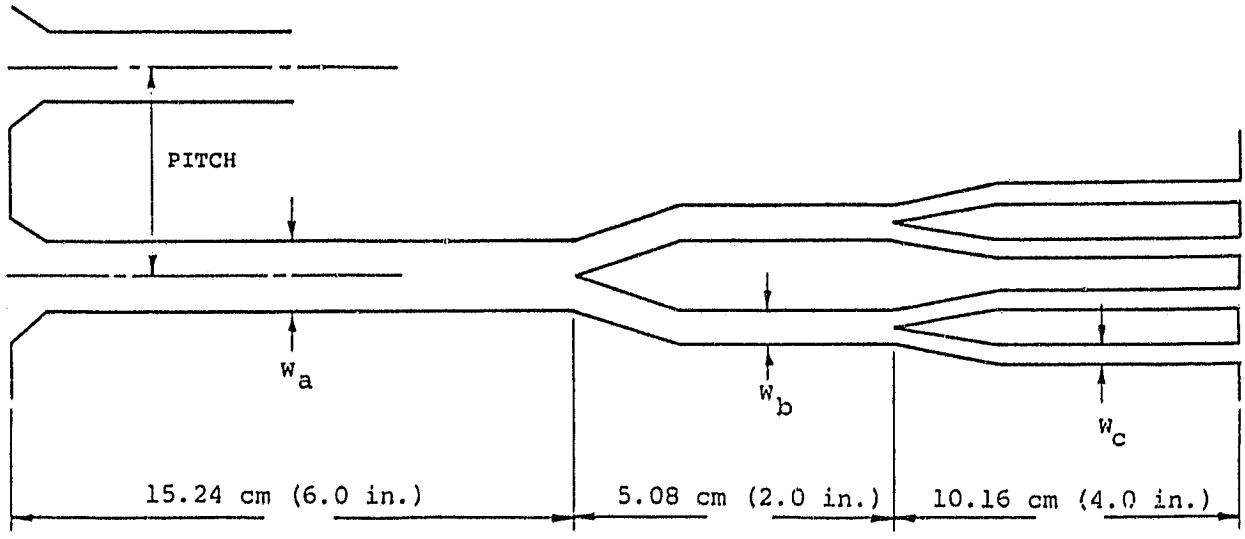

D1575R

	DESIGN		
	4DT/4ZT	5DT	5ZT
w_a	0.508 cm	0.569 cm	0.635 cm
w_b	0.254 cm	0.284 cm	0.318 cm
w_c	0.127 cm	0.142 cm	0.159 cm
Pitch	1.257 cm	1.323 cm	1.270 cm

FIGURE 4.1 CHANNEL GEOMETRY FOR 'TREE' DESIGNS

(All dimensions are before heat treatment; DT: DIGAS with straight cooling; ZT: separated cooling with 'tree' channels; numbers 4 or 5 indicate 4 or 5 cells per cooling plate)

cell temperature close to the maximum temperature within the cell. Therefore, the logical basis for a comparison of all cooling geometries was to assume the same peak temperature. The parasitic losses considered for comparing different designs include only the process and cooling air flows and their respective pressure drops through the stack itself. The net voltage for each design was estimated from a calculated performance at 177°C (average temperature) after correcting for ΔV_a, voltage loss equivalent to auxiliary power loss, and ΔV_t, voltage adjustment due to operation at an average temperature different from 177°C. The atmospheric test data (6), showing an output voltage change of about 1.35 mV for each °C change in the stack temperature at 300 mA/cm^2, was utilized in calculatint ΔV_t.

Table 4.1 shows the calculated mean temperature, corrections ΔV_t and ΔV_a, and the net voltage for six different designs, namely 4DS, 5DS, 4DT, 5 DT, 4ZT and 5 ZT. The number 4 or 5 indicates 4 or 5 cells per cooling plate. The designation DT indicates DIGAS with 'tree' cooling, DS indicates DIGAS with straight cooling channels, and ZT indicates separated cooling with 'tree" channels. The net voltages of the straight through DIGAS designs are 20 to 30 mV below those of the 'tree' DIGAS designs due exclusively to the higher temperature gradient. Separated air cooling provides an additional 22 mV owing to a higher oxygen partial pressure. The net voltage for designs with 4 or 5 cells per cooling plate is quite similar and, therefore, 5 cells per cooling plate were selected for the final design.

This analysis establishes the configuration 5ZT, i.e., the separated air cooling design with five cells per cooling plate to be better than other configurations. This design was therefore incorporated in the pressurized stack testing. Several gas cooled fuel cell stacks, including one of a 10 kW size, were tested at pressures up to 1010 kPa (10 atm) to study the effectiveness of gas cooling. The separated cooling

TABLE 4.1 COMPARISON OF DIFFERENT COOLING PLATE DESIGNS*

Cooling Plate Design	4DS	5DS	4DT	5DT	4ZT	5ZT
Calculated Performance at $\bar{T}$ = 177°C, mV	551	552	552	552	574	574
Avg. Temperature $\bar{T}$, °C to maintain T_{max} at 190°C	163	156	180	178	185	185
ΔV_t, mV† ‡	18.9	-28.4	+4.1	+1.4	+10.8	+10.8
ΔV_a, mV†	-3.6	-4.3	-3.3	-3.3	-2.8	-2.3
Net Voltage, mV	529	519	553	550	582	583

*Pressure: 345 kPa; Bulk Air Temperature Rise: 55°C; Makeup Air Flow: 2 Stoich; Fuel Utilization: 70%

†Cell voltage corrections for operation at fixed maximum temperature T_{max} = 190°C (ΔV_t) and for power loss due to stack pressure drops at a current density of 300 mA/cm^2 (ΔV_a).

‡Assume voltage change of 1.35 mV/°C, based on atm. pressure data. Note that pressurized data reported in the next section indicated ∿2 mV/°C. The relative comparisons, however, remain unchanged.

is better than the DIGAS on the temperature uniformity and net performance basis, and additional technological issues such as moldability of the plate design, acid management, etc. are currently being resolved.

4.3 DESIGN AND ASSEMBLY OF THE 10 kW AIR-COOLED STACK (P10-1)

Stack P10-1 (a 50 cell 12"x17" stack) was designed to operate at pressures between 101 kPa and 690 kPa. This stack incorporated machined 'Z' bipolar and 'tree' cooling plates, floating manifolds and Acid Fill Scheme AF-2 (6). The design details of this stack are shown in Figure 4.2. Belleville springs were incorporated to prevent a loss of stack compression with time. The components of the stack consisted of standard cathodes ($\sim$0.5 mg Pt/cm^2), anodes ($\sim$0.3 mg Pt/cm^2), and Mat-1 matrices. The stack was wet assembled with 50 ml of approximately 96 wt% phosphoric acid (an additional 0.5 cc in each reservoir) and compressed with a holding pressure of 445 kPa. A photograph of the assembled stack without the manifolds is shown in Figure 4.3.

4.4 TESTING OF STACK P10-1

This stack was tested at pressures of 101 to 690 kPa. The test results are given below.

- TESTING AT ATMOSPHERIC PRESSURE: The stack was pretested at atmospheric pressure and all the cells performed satisfactorily. The tests conducted were:
  - gas tightness,
  - stable and transient OCV, and
  - performance at 150 mA/cm^2.

  The cell edge and the manifold seals were tested under a hydrogen back pressure of 13 cm of water and almost no hydrogen leak was detected. The OCV tests also indicated a cross-leak tight stack. Although the stack was assembled with a lower concentration of acid, the initial performance of all the cells at $\simeq$ 150 mA/cm^2 was acceptable (Figure 4.4). Somewhat lower performance of the cells

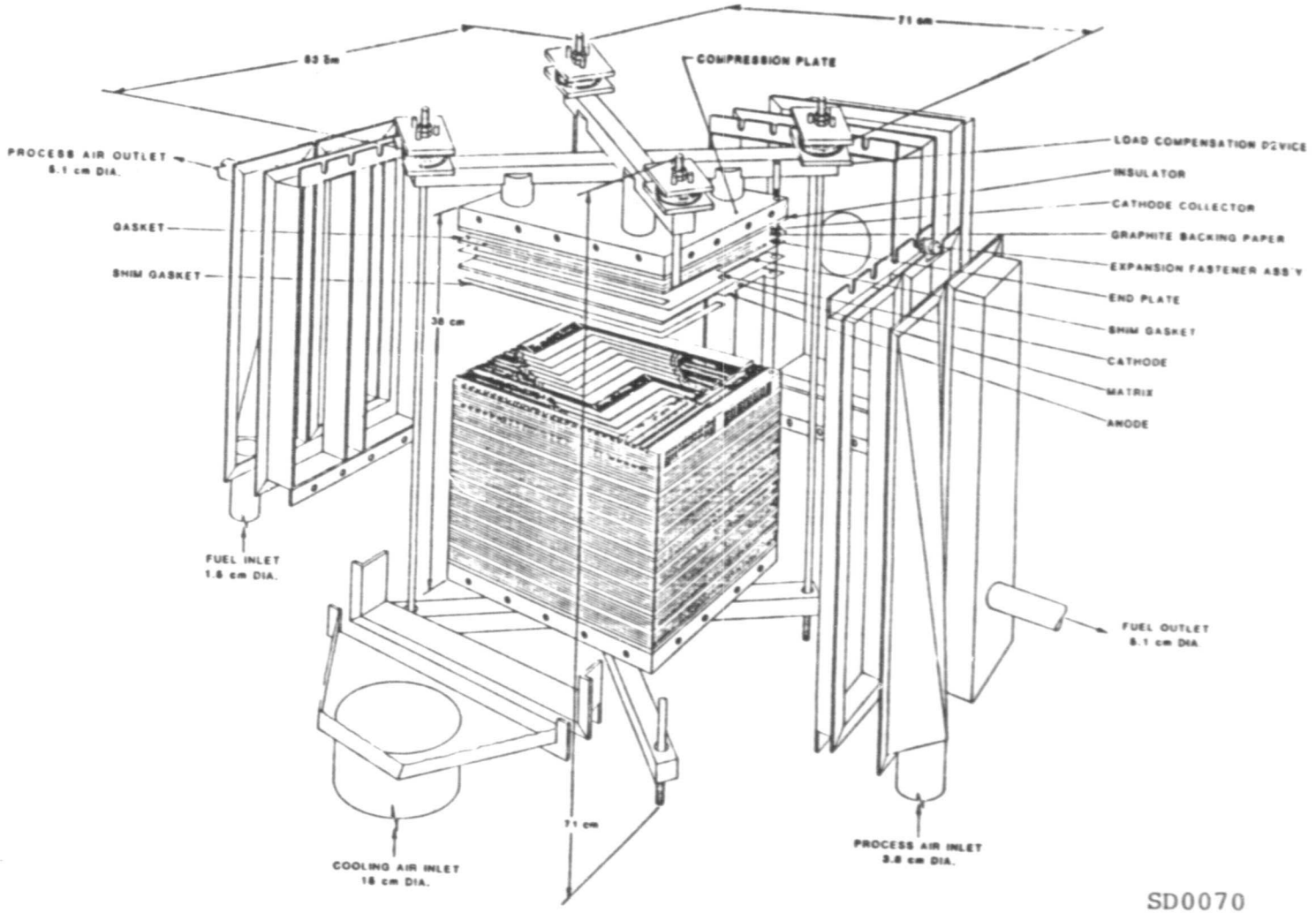

FIGURE 4.2 TWO-POINT PERSPECTIVE DRAWING OF THE 10 kW STACK (P10-1)

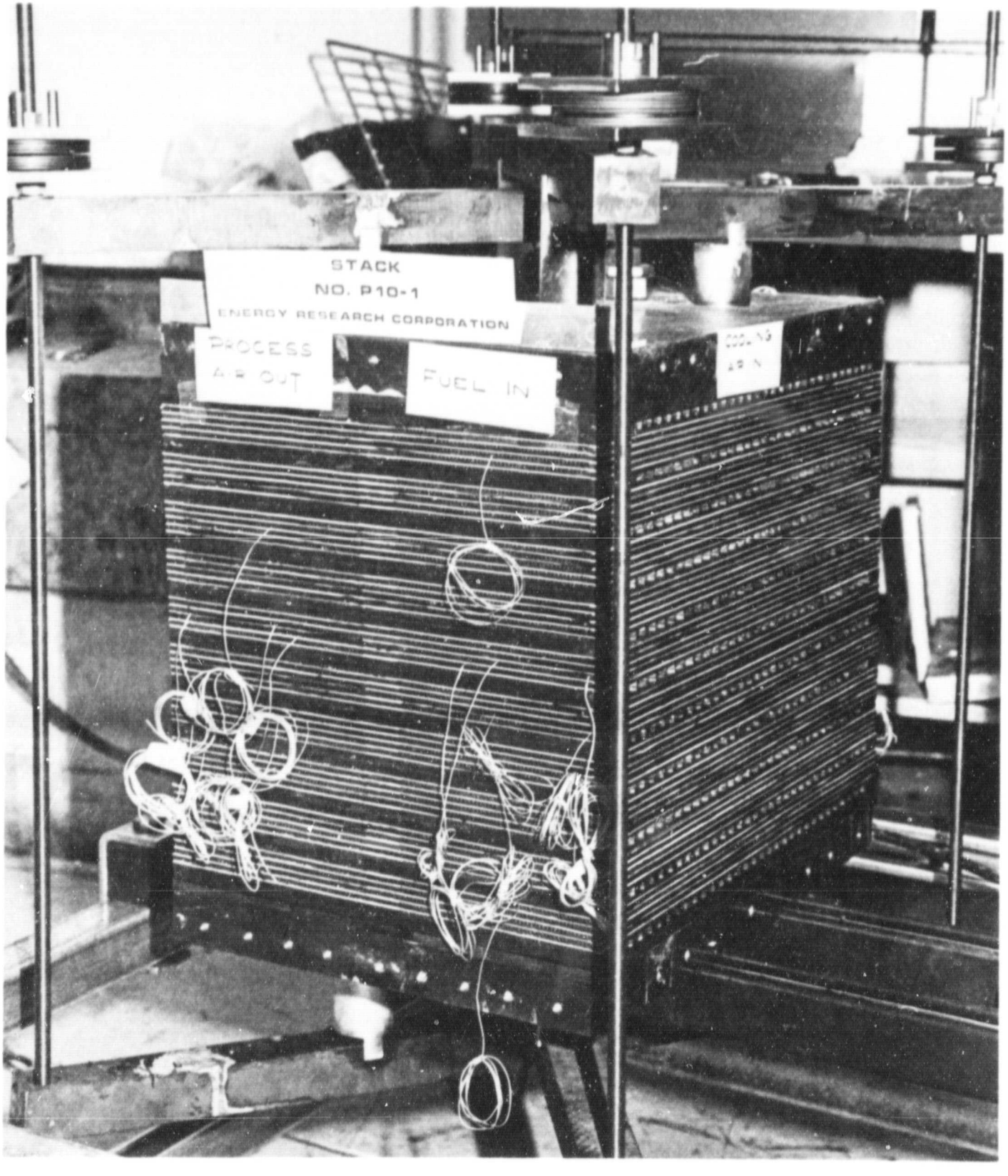

FIGURE 4.3 ASSEMBLED STACK P10-1 (50-CELL)

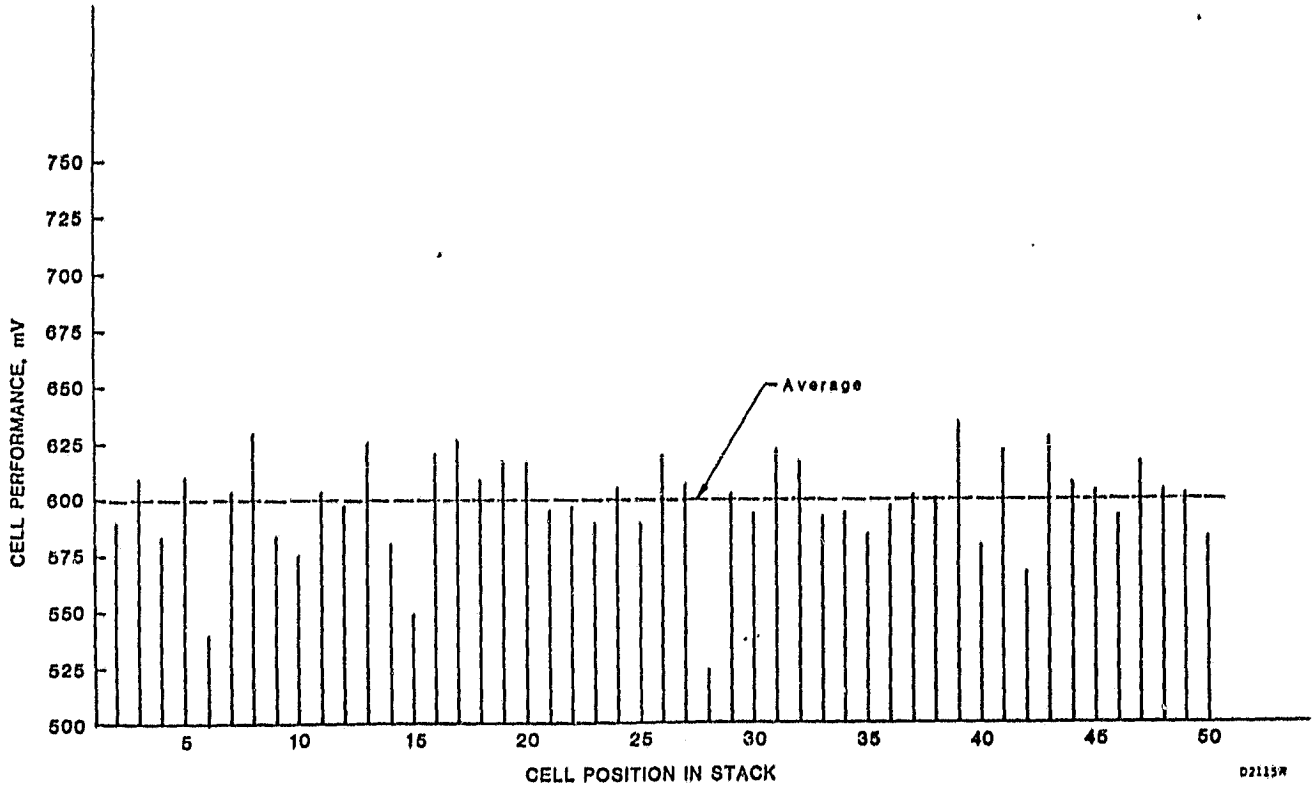

FIGURE 4.4 INITIAL PERFORMANCE OF STACK P10-1 AT ATMOSPHERIC PRESSURE (Current Density: 150 mA/cm^2; Maximum Stack Temperature: 186°C; Air Util.: 60%; Fuel Util.: 77%; Fuel: Pure H_2; Stack Resistance: 0.27 mΩ/Cell)

is due to a less than optimum wetting of the cells at the time of testing.

- TESTING AT PRESSURE: Testing of Stack P10-1 was performed at Westinghouse (Pittsburgh, Pa) facilities and included:

  1. An open circuit voltage and a low load (20 A at 150°C) performance checkout at atmospheric pressure;

  2. Performance testing as a function of stack temperature (175, 180 and 190°C), coolant inlet temperature (125, 140 and 150°C), air utilization (33 and 50%), current density (between 100 and 400 mA/cm^2) and pressure (345, 515 and 690 kPa);

  3. About 24 hours of continuous operation at 325mA/cm^2, 515 kPa, 190°C stack, 140°C coolant inlet temperature and 2 stoich air; and

  4. About 500 hours of continuous operation at 325 mA/cm^2, 690 kPa, 190°C stack maximum temperature, 140°C coolant inlet temperature and 2 or 3 stoich air.

  All 50 cells showed an excellent performance at the beginning of the atmospheric checkout testing at Westinghouse. However, some water accumulation in the cathode exhaust manifold, during the initial atmospheric test period, resulted in a reversal of the bottom five cells of the stack. Because permanent damage to these cells was suspected, this 5-cell pack was shorted by taking advantage of the structure of the cooling plates. This resulted in Stack P10-1 having only 45 active cells instead of 50 as originally intended. Following this correction, atmospheric testing resumed and all 45 remaining cells showed an excellent performance. Next, the stack was tested at three different pressures. The performance mapping data at different pressures is given in Appendix B. A few test interruptions occurred due to compressor failure, power interruptions, etc.

The test results, data analysis and effect of these interruptions on the cell performance are discussed in the next section.

TASK 5. DATA ANALYSIS

The test results of the 10 kW size gas cooled stack reported in the previous section were analyzed to investigate the following aspects:

- Thermal response of the pressurized gas-cooled PAFC stacks
- Performance of the stack at different pressures
- Parasitic power loss requirement
- Water distribution in the exhaust streams
- CO related performance loss at pressure
- Effect of steady state operation and operating upsets on the pressurized PAFC performance.

5.1 THERMAL RESPONSE OF GAS-COOLED PAFC STACKS

The average temperature of the stack was varied by changing the cooling air inlet temperature and flow rate while holding all other variables at constant values. As shown in Figure 5.1, the effect of the average cell temperature on the pressurized fuel cell performance is current density dependent as was also observed in atmospheric pressure cells. However, the effect of the average temperature on the fuel cell performance was somewhat greater at pressure than at atmospheric pressure, ranging from 1.2 mV/°C at 150 mA/cm^2 to 2 mV/°C at 300 mA/cm^2, at pressures of 345 to 690 kPa. Note that the pressurized operation increases the mV/°C factor by 1.5 $\frac{R}{F}$ lnP. Thus an additional 0.2 mV/°C is expected at 5 atm pressure because of this term.

The difference between the maximum to average temperature ($T_{max} - \bar{T}$) is a logical measure of temperature uniformity and is desired to be as low as possible. The data indicated that the ($T_{max} - \bar{T}$) is independent of the operating pressure, but is a function of current density and coolant temperature rise. The experimental ($T_{max} - \bar{T}$) values agreed reasonably well with the

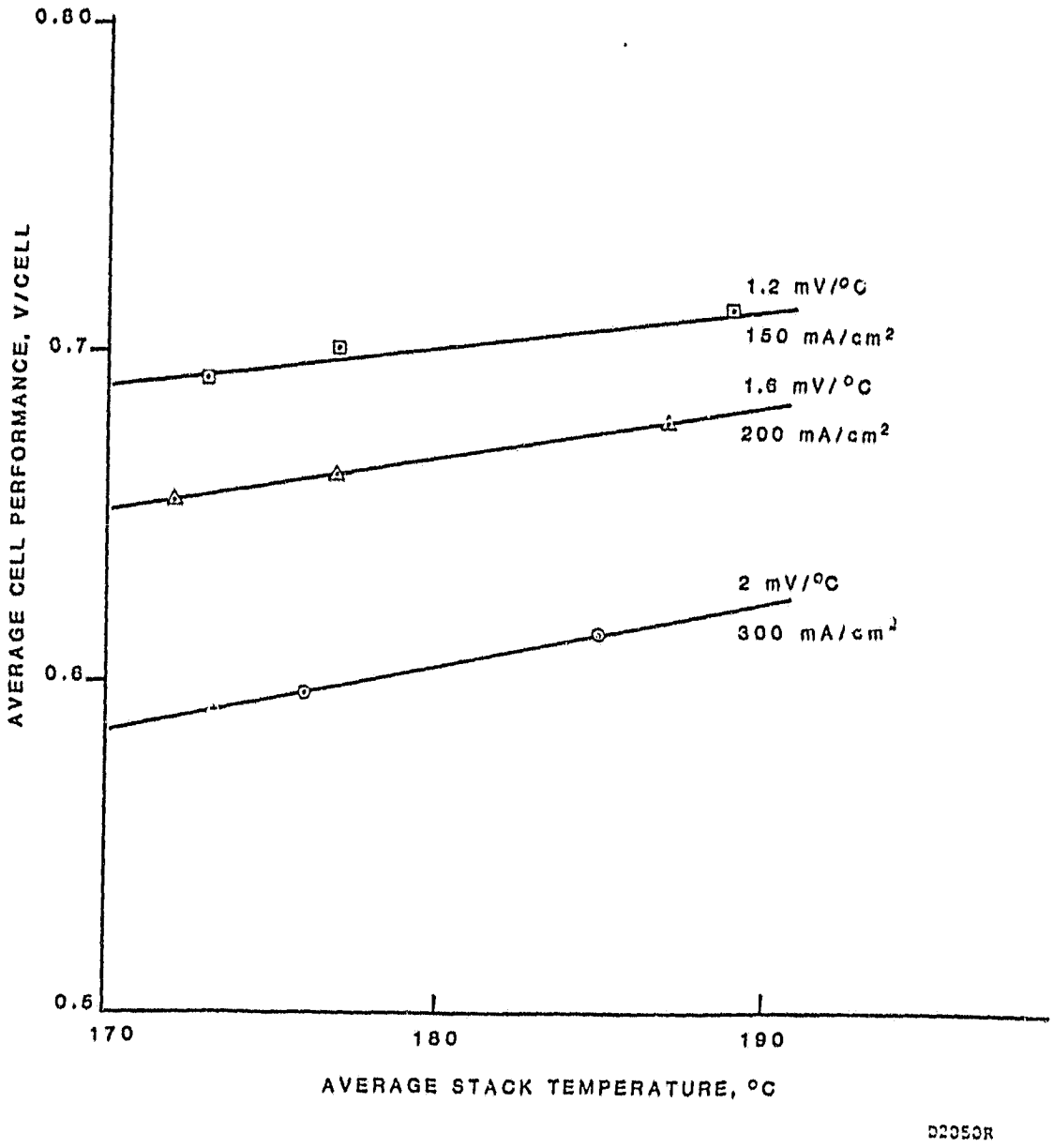

FIGURE 5.1 EFFECT OF TEMPERATURE ON PERFORMANCE OF THE 10 kW STACK (515 kPa; 50% Air Util.; 40% Fuel Util.)

predicted values. For test conditions ranging from 345 to 690 kPa and 100 to 400 mA/cm^2, $(T_{max} - \bar{T})$ stayed below 19°C for a coolant temperature of <75°C (results of 30 test runs are summarized in Table 5.1). The experimental temperature ratio index r, a measure of temperature uniformity, defined as:

$$r = \frac{(T_{max} - \bar{T})_{stack}}{(T_{out} - T_{in})_{cooling}}$$

for these test conditions, is plotted in Figure 5.2 as a function of current density. The figure also shows the predicted values of r for a cooling air ΔT of 30°C. The measured values of r are higher than predicted at higher current densities. However, the agreement between measured and predicted uniformity appears to be reasonably good; most measured values of r are within 30% of the predicted values. The cooling air ΔT calculated from the heat generation and corrected for heat removed by the process air, agreed reasonably well with the experimental values (except for a few tests with a high cooling air ΔT), suggesting a good thermal balance for the pressurized fuel cells.

The measured and predicted temperatures for the stack operating at a power output of 0.2 W/cm^2 (at 515 kPa and 325 mA/cm^2) are shown in Figure 5.3. For this case, the $(T_{max} - \bar{T})$ value was predicted to be 9°C and the measured value was 11°C. The design analysis also accurately predicts the temperature rise trend (in the coolant flow direction) in the fuel inlet-process air outlet edge, center and process air inlet-fuel outlet edge regions. The process air inlet-fuel outlet edge temperatures (right hand side of Figure 5.3) are generally lower than the fuel inlet-process air outlet edge. This is because the process air inlet-fuel outlet edge has a lower current density and an additional cooling, due to incoming process air. It appears that the temperature distribution can be improved by omitting one cooling channel at the fuel inlet-process air outlet edge, and two channels at the process air inlet-fuel outlet edge.

TABEL 5.1 THERMAL PERFORMANCE OF A 1.0 kW STACK AT PRESSURE

TEST PRESSURE	i CURRENT DENSITY mA/cm^2	$\bar{T}$ AVERAGE CELL TEMPERATURE °C	$T_{max} - \bar{T}$ MAXIMUM TO AVERAGE TEMPERATURE RISE, °C	ΔT_{CA} COOLING TEMPERATURE RISE, °C		$r = \frac{T_{max} - \bar{T}}{\Delta T_{CA}}$ TEMPERATURE UNIFORMITY RATIO
				Measured	Calculated	
	100	174	7.2	33	44	0.22
	125	173	7.7	28	32	0.28
	150	174	7.4	27	31	0.27
	175	174	8.8	26	29	0.34
	200	174	8.0	23	25	0.35
345 kPa	300	178	9.5	24	28	0.40
	300	189	12.1	34	37	0.36
	300	188	16.4	34	39	0.48
	150	193	17.9	74	101	0.24
	200	191	16.6	68	94	0.24
	300	192	18.3	50	59	0.37
	350	191	19.8	47	54	0.42
	400	188	13.5	40	42	0.34
	150	179	8.6	34	37	0.25
	200	178	7.7	29	35	0.26
	250	178	8.3	29	41	0.29
	300	177	8.2	23	24	0.36
515 kPa	100	175	7.3	38	58	0.19
	150	174	6.8	29	32	0.23
	200	174	8.3	26	32	0.32
	250	173	7.5	22	25	0.34
	325	184	9.8	28	31	0.35
	100	190	12.9	53	51	0.25
	200	188	12.7	48	50	0.26
	300	187	12.3	35	36	0.35
	350	185	9.8	27	29	0.36
690 kPa	150	196	27.6	84	80	0.33
	200	191	16.1	71	72	0.23
	300	189	16.5	50	50	0.33
	350	189	15.9	48	54	0.33

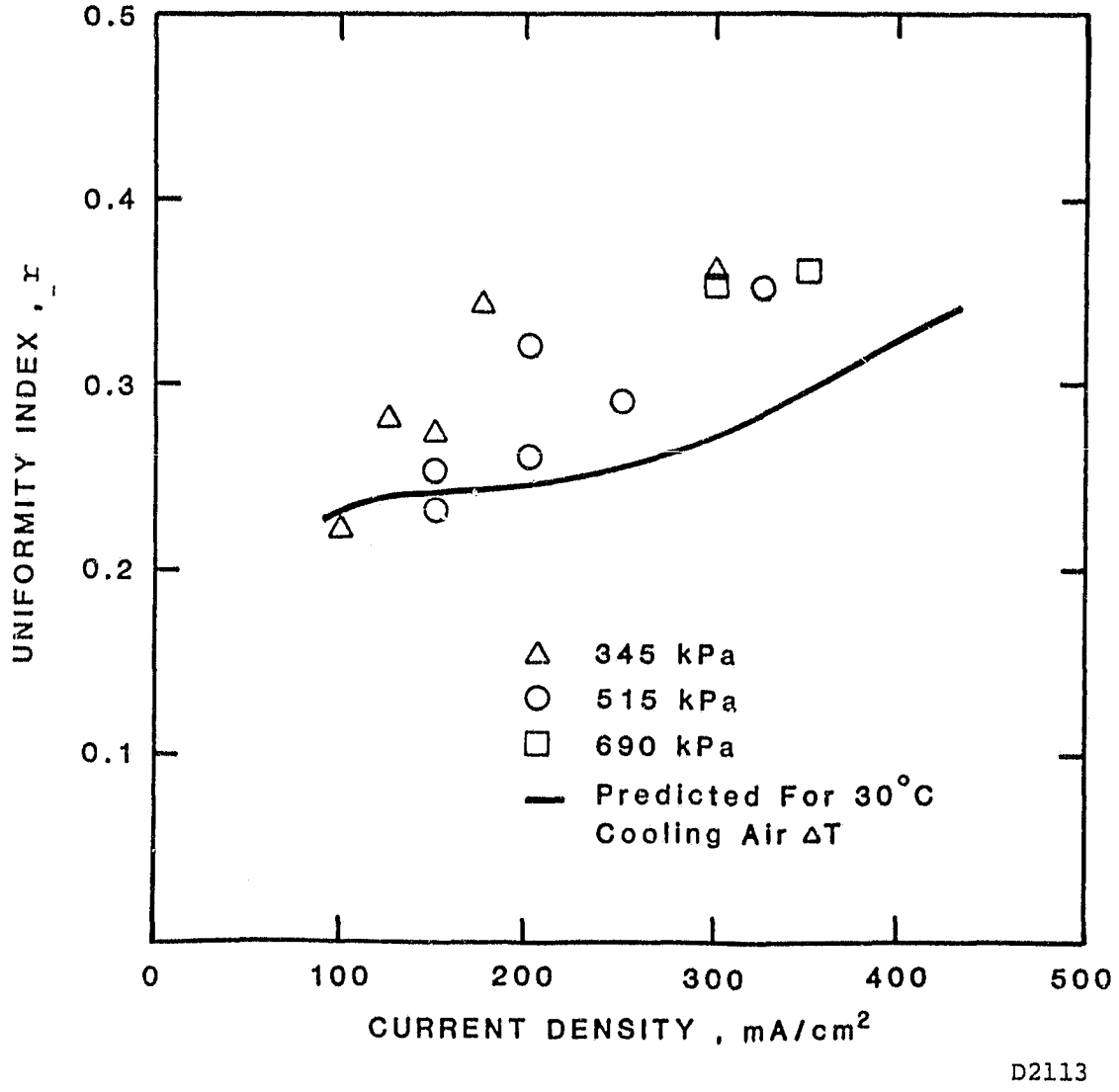

FIGURE 5.2 TEMPERATURE UNIFORMITY INDEX, r, VS. CURRENT DENSITY (Air Util.: 50%; Fuel Util.: 40%; 30 ± 5°C Coolant Temperature Rise)

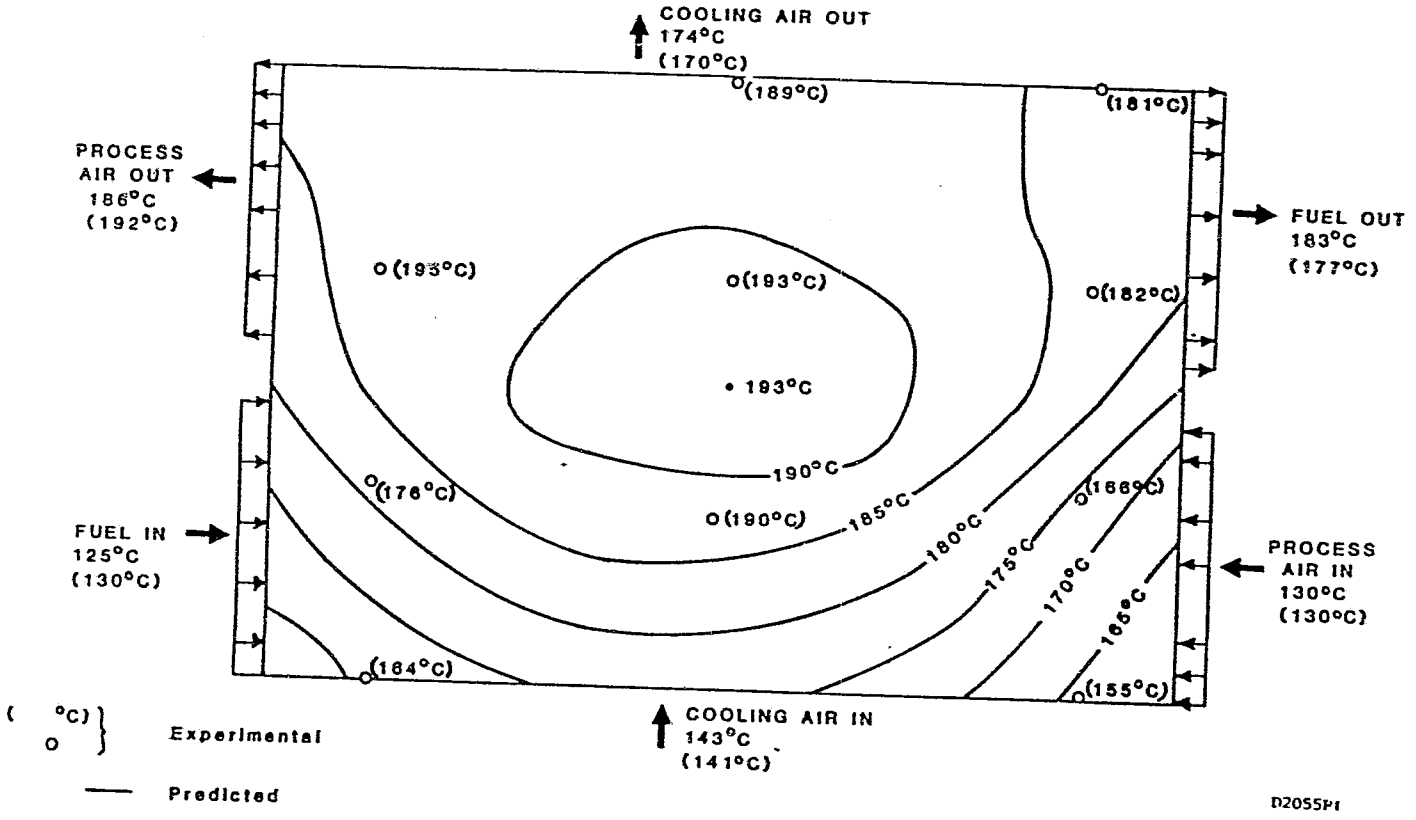

Max. Cell Temp.=193 (195°C)
Min. Cell Temp.=164 (155°C)
Avg. Cell Temp.=184.00 (184°O)
Max. - Avg.. Temp.=9°C (11°C)

Cell Voltage= 0.604V (0.605V)
Current Density=325 mA/cm²
Pressure=515 kPa
Fuel Utilization=0.40
Air Utilization=0.50

FIGURE 5.3 COMPARISON OF A PREDICTED AND EXPERIMENTAL TEMPERATURE PROFILE IN A TYPICAL CELL OF A 10 kW STACK (The experimental measurements are shown in parentheses)

5.2 EFFECT OF CURRENT DENSITY ON CELL PERFORMANCE

Performance of the 10 kW (1200-cm^2 cell area) stack at two different pressures is reported in Figure 5.4. At 515 kPa and 300 mA/cm^2 ($\bar{T}$ = 184°C), the stack performance was 0.614 V/cell (i.e., 0.19 kW/cell) which corresponds to an energy conversion efficiency of 49% (based on lower heating value of H_2) in the PAFC stack. As reported in the previous section, the performance gain obtained by raising the pressure from P_1 to P_2 (Table 5.2) was somewhat higher than the theoretical values.

5.3 PRESSURE DROP AND PARASITIC POWER REQUIREMENT

Pressure drops were measured in different streams as a function of pressure. The pressure drops through the cathode, anode, and cooling channels corresponding to a 325 mA/cm^2 and 515 kPa operation were 4 mm Hg (50% air utilization), 1 mm Hg (80% fuel utilization), and 5 mm Hg, respectively. The pressure drop decreased with the operating pressure. Experimental results confirmed that the pressure drop is inversely proportional to the operating pressure (Figure 5.5).

The parasitic power corresponding to the pressure drop through the stack was calculated for different power level operations at 515 kPa and is presented in Figure 5.6. An adiabatic compression at an 80% blower efficiency was assumed. The parasitic power requirements related to the cooling and process air pressure drops at 325 mA/cm^2 and 515 kPa are quite negligible, 0.9 and 0.2% of the output power, respectively. (These values only account for a pressure drop through the fuel cell stack and the manifolds.) Note that the pressure drop related parasitic power loss is inversely proportional to the operating pressure.

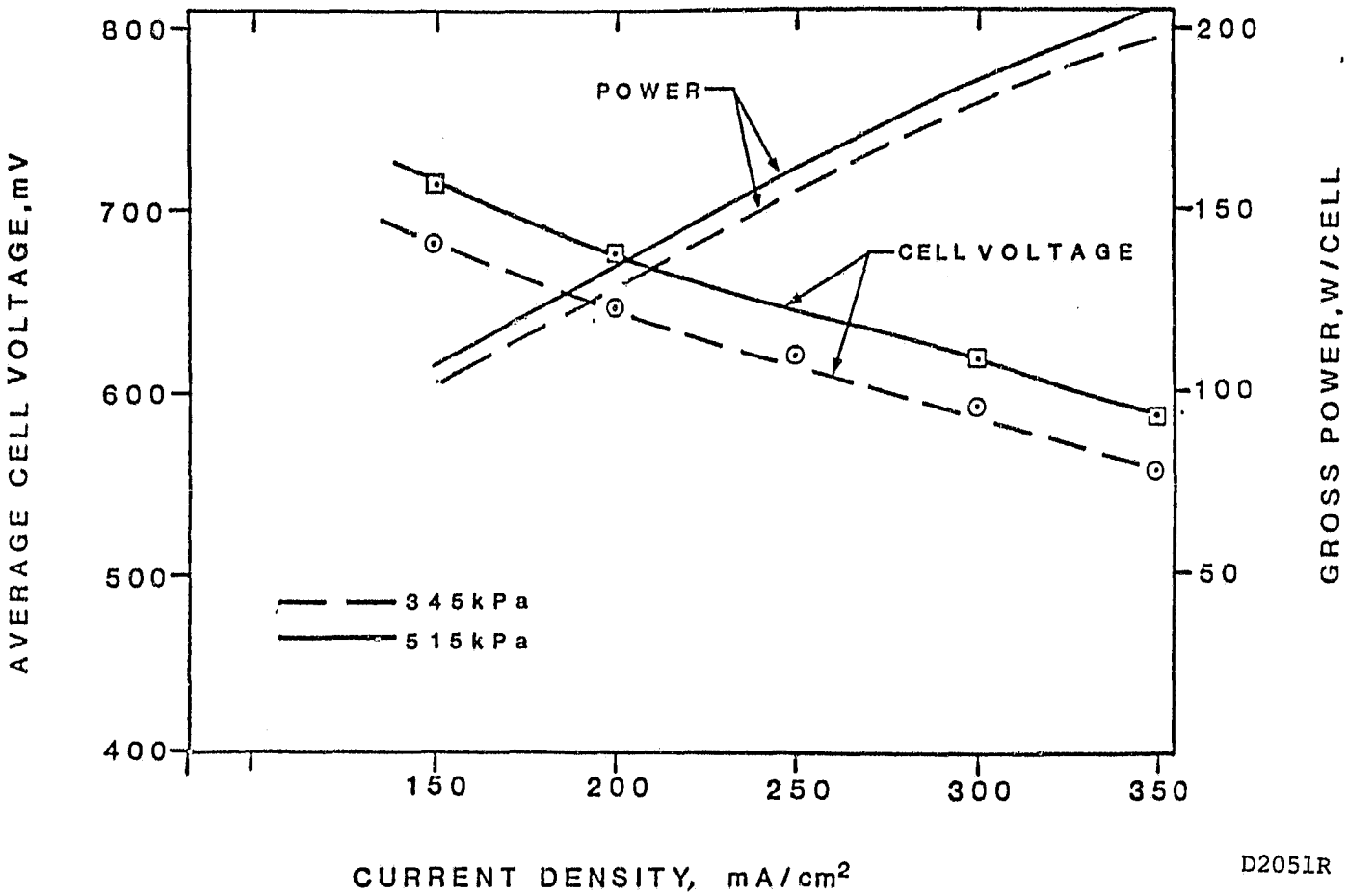

(FUEL COMPOSITION: 80.8% H_2, 15% CO_2, 1.5% CO, 3.7% H_2O
FUEL UTILIZATION: 40%;
OXIDANT UTILIZATION: 50%;
AVERAGE TEMP VARIED BETWEEN 184°c & 189°c;
COOLANT INLET TEMPERATURE: 140°c)

FIGURE 5.4 PERFORMANCE OF THE 10 kW STACK AT TWO DIFFERENT PRESSURES

TABLE 5.2 AVERAGE PRESSURIZED PERFORMANCE GAIN, 10 kW STACK (@ 150 mA/cm^2)

PRESSURIZATION STEP, kPa	AVERAGE STACK TEMP., °C	THEORETICAL GAIN $1.5 \frac{RT}{F} \ln P_2/P_1$ mV	AVERAGE STACK GAIN mV/CELL
101 - 315	175	75	83
315 - 515	177	24	28
515 - 690	186	17	31

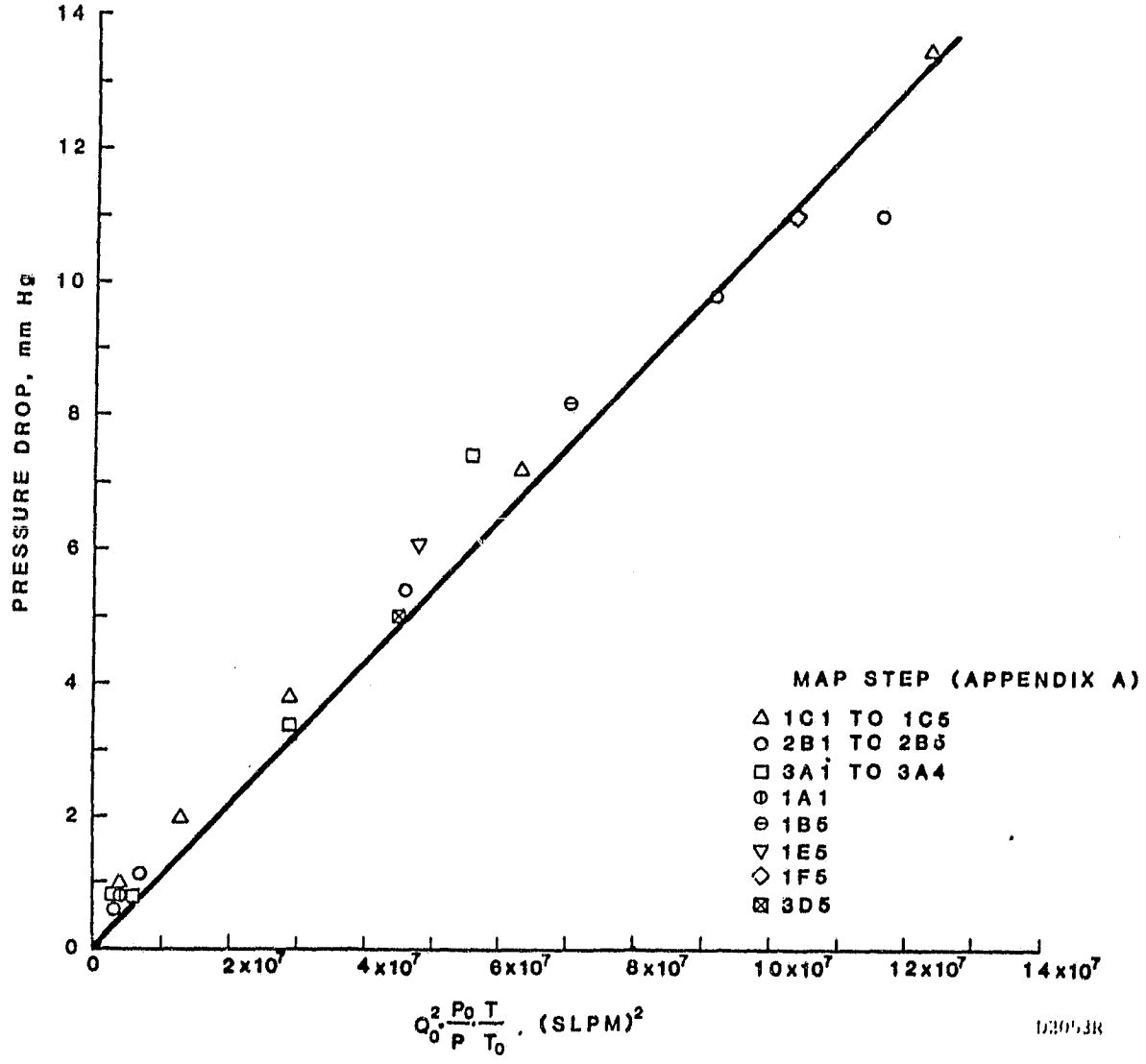

FIGURE 5.5 COOLING SIDE PRESSURE DROP AS A FUNCTION OF OPERATING PRESSURE (Stack P10-1: Ten 'tree' coolers; Q_o: Standard Flow, lpm; P_o: Standard Pressure; T_o: Standard Temperature; T: Operating temperature; P: Operating Pressure)

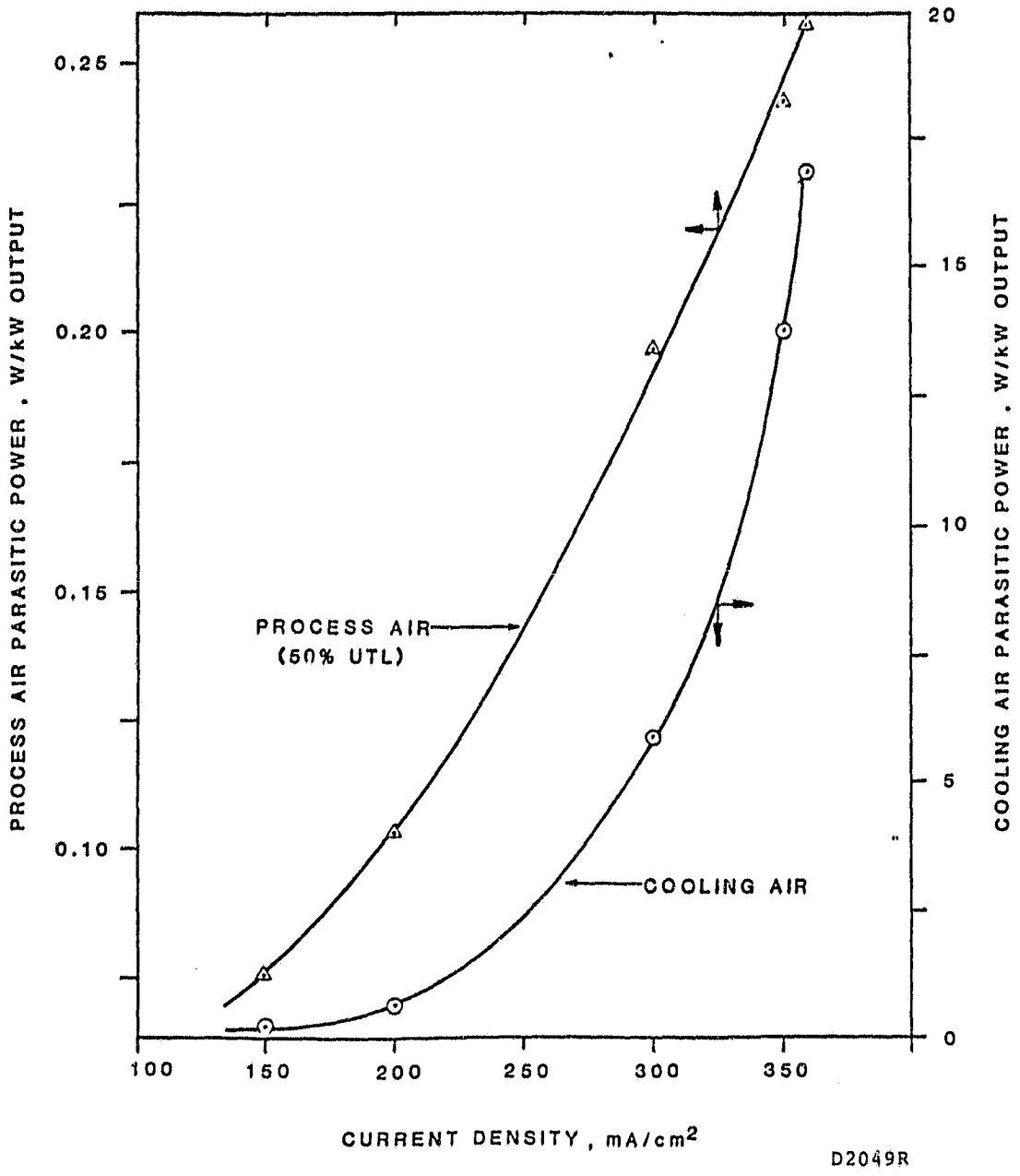

FIGURE 5.6 COOLING AND PROCESS AIR CONTRIBUTION TO PARASITIC POWER CONSUMPTION, 10 kW STACK (515 kPa Operation; coolant inlet temperature: 140°C; Air Inlet Temperature: 130°C; Stack Average Temperature: 183-180°C; Air Utilization: 50%; Fuel Util.: 40%)

5.4 WATER BALANCE

The water concentration in the exhaust stream has important implications on the fuel cell design, acid concentration profile and water recovery from the exhaust gases. The water partial pressures in the anode and cathode exit streams, and the percentage of the product water transferred to the anode stream, were calculated corresponding to different operating conditions, using water collection rates at the anode and cathode (Table 5.3). For the separated air-cooled stacks with counter-current reactant flows and 50% air utilization, the water partial pressure in the cathode exhaust stream is roughly two times higher than the anode stream and 17 to 18% in the cathode stream at pressure (515 to 690 kPa). Total water collected at different conditions plus the water input to the stack with the reactants matched with the water produced in the fuel cell.

5.5 EFFECT OF CARBON MONOXIDE ON PERFORMANCE

The CO related performance loss for the pressurized fuel cell was 6 mV (184 to 189°C average temperature, 40% fuel utilization) for a 1.5% CO content. The CO related performance loss was also observed to be independent of the operating pressures, suggesting the CO-related poisoning to be concentration rather than activity related.

5.6 STEADY STATE OPERATION AT PRESSURE

The performance of Stack P10-1 at 515 kPa, 325 mA/cm^2 and 184°C (average stack temperature) is shown in Figure 5.7. The average fuel cell performance was 0.600 V/cell which corresponds to a thermal to electrical efficiency of 48% in the fuel cell stack. The power output of the 45-cell stack at this condition was 9.4 kW.

Stack P10-1 was also run at 690 kPa and 325 mA/cm^2 for a total of 465 hours. The test history and the stack performance

TABLE 5.3 WATER BALANCE FOR A PRESSURIZED SEPARATED AIR-COOLED STACK

(10 kW Stack; Average Stack Temperature: $\sim$185°C; Fuel Compotision: 80.8% H_2, 15% CO_2, 1.5% CO, 3.7% H_2O; Fuel Utilization: 40%)

OPERATING CONDITION		WATER IN THE EXIT STREAM		% REACTION WATER TRANSFERRED TO THE ANODE STREAM
PRESSURE kPa	AIR UTIL. %	CATHODE %	ANODE %	
515	50	18	7	4
690	50	17	8	6
690	33	12	7	4

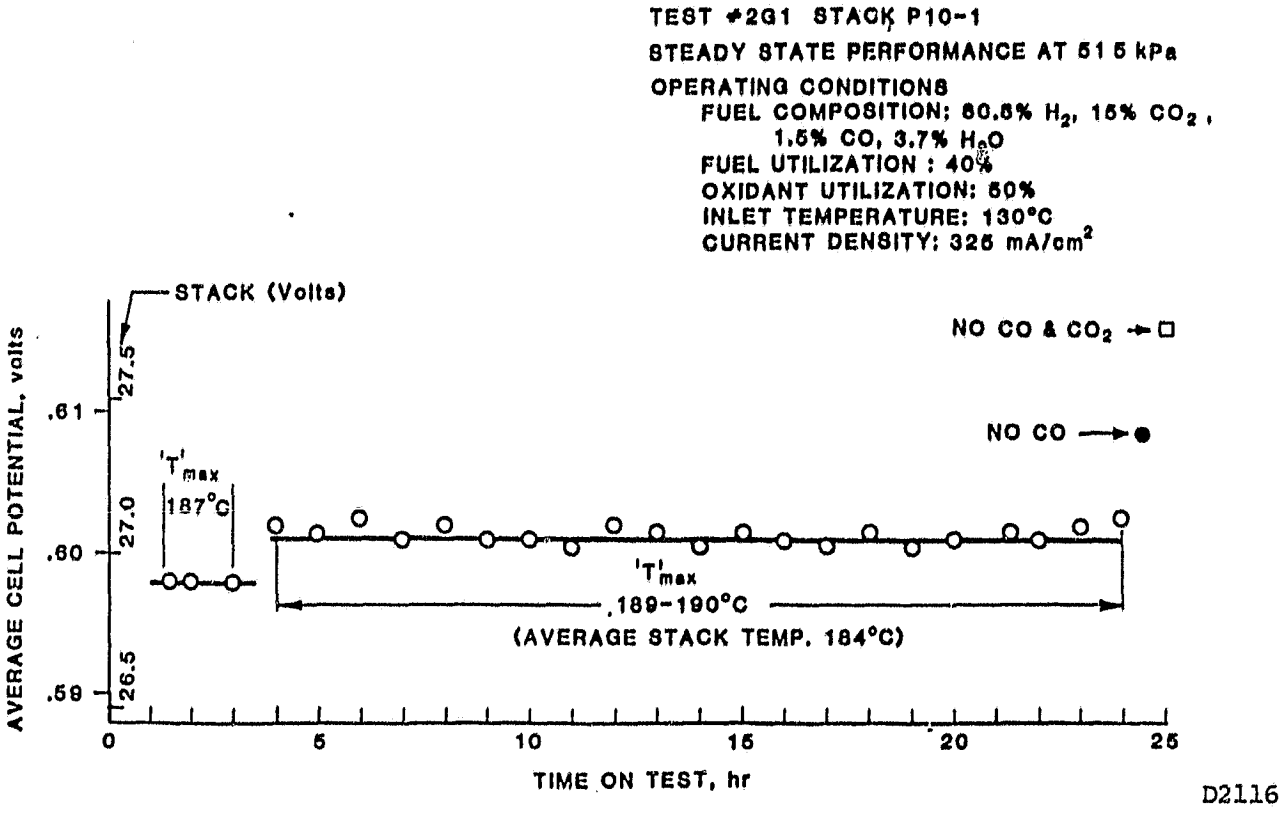

FIGURE 5.7 PERFORMANCE OF STACK P10-1 AT 325 mA/cm^2 AND 515 kPa

is reported in Figure 5.8. During this test, the stack was subjected to one H_2 supply outage and two power failure related shutdowns (full depressurization pressurization). These tests indicated a performance loss of 14 mV/cell during the H_2 outage related test (the fuel cell was kept at open circuit at 190°C, 690 kPa for a total of about 12 hours) and about 8 mV/cell during each of the power failure related shutdowns. It may be noted that during performance mapping tests at 515 kPa the stack was subjected to three additional pressurization-depressurization cycles. During each of these depressurization runs, the wet seals of the cells in the coolant inlet and outlet edges were exposed to large differential pressure variations (over $\simeq$35 kPa pressure) and withstood these large ΔP variations without much harmful effect to the fuel cell performance, indicating an acceptable differential pressure capability of the present wet-seal design.

During the initial 300 hours of steady-state pressurized operation, the stack resistance stayed constant at $\simeq$0.25 mΩ/cell. However, after the cathode flow rate was increased to 33% air utilization, a gradual increase in the cell resistance was observed, indicating a need for acid addition. The cathode and anode terminal resistances were $\simeq$ 1 and 2 mΩ, respectively, and stayed somewhat constant during the testing.

The testing of this stack was voluntarily discontinued after a total of 685 hours of pressure testing at different conditons.

5.7 SUMMARY OF THE 10 kW STACK DATA ANALYSIS

The feasibility of gas cooling for the pressurized PAFC was established through the successful testing of a 10 kW separated air-cooled stack at different pressures for $\simeq$700 hours. Using one 'treed' cooler every five cells, the stack produced 0.2 W/cm^2 at 515 kPa and 325 mA/cm^2 while maintaining a uniform temperature distribution (the maximum to average temperature difference was found to be only 11°C).

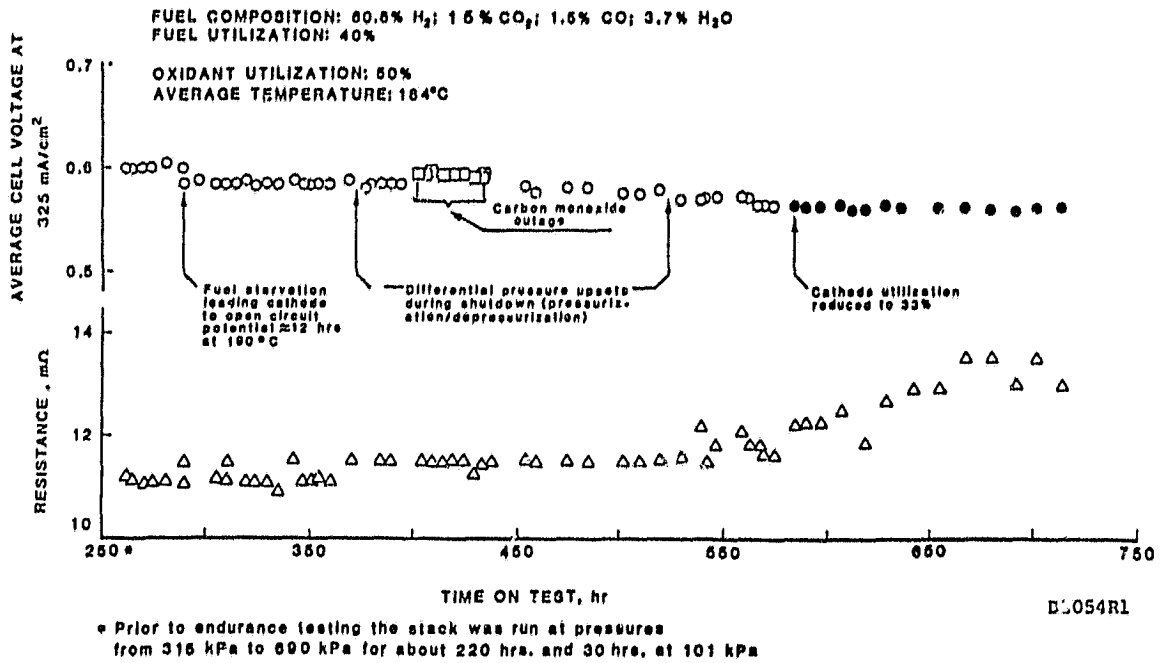

FIGURE 5.8 PERFORMANCE OF THE 10 kW STACK AT 325 mA/cm^2 AND 690 kPa

The pressure testing of the 10 kW stack also indicated that:

- The effect of air flow and CO concentration on fuel cell performance, temperature distribution and temperature uniformity of a fuel cell are independent of operating pressure.
- The effect of the average temperature on performance is greater for a pressurized cell as compared with an atmospheric pressure cell.
- The pressure drop through the process and cooling channels is inversely proportional to pressure and the total parasitic cathode and cooling power dissipation through the stack at 516 kPa (325 mA/cm^2) is less than 1% of the output power.

REFERENCES

1. Maru, H.C. and Baker, B.S., "Fuel Cells for Utility Applications - a Refreshing Approach," International Power Generation, February, 1981.

2. Warshay, M., Prokopius, P., Simons, S. and King, R.B., "Commercial Phosphoric Acid Fuel Cell System Technology Development," 14th Intersociety Energy Conversion Engineering Conference, Vol. 1, Paper No. 538, American Chemical Society, Washington, DC, 1979.

3. Maru, H.C., Chi, C., Patel, D. and Burns, D., "Heat Transfer in Phosphoric Acid Fuel Cell Stacks," 13th Intersociety Energy Conversion Engineering Conference, Paper No. 789281, Society of Automotive Engineers, Inc., Warrendale, PA, 1978.

4. Maru, H.C., "Electrochemical Cell Operation and System," U.S. Patent No. 4,192,906, March 11, 1980.

5. Kothmann, R.E., "Fuel Cell System Configurations", U.S. Patent No. 4,276,355, June 30, 1981 (Assigned to U.S. Government).

6. Hoover, D.Q., Jr., "Cell Module and Fuel Conditioner Development," Final Report, DOE/NASA Contract No. DEN3-161, (NASA CR-165193), February, 1983.

7. Christner, L., "Technology Development by Phosphoric Acid Fuel Cell Powerplant (Phase II)," Final Report, DOE/NASA Contract DEN3-67, (NASA CR-165426), December, 1981.

8. MacDonald, D.I. and Boyack, J.R., "Density, Electrical Conductivity and Vapor Pressure of Concentrated Phosphoric Acid," J. Chem. Engrg. Data 14, 330 (1969).

APPENDIX A. NUMERICAL DATA ON ACID CONCENTRATION CHANGES

PRESSURE atm	TEMPERATURE, °C	ACID CONCENTRATION, wt% H_3PO_4	ACID VOLUME, ml/gm of H_3PO_4	% Volume Change from 100 wt% & 180°C H_3PO_4
1	120	93.87	.63	9.12
1	140	96.74	.60	4.75
1	160	98.87	.58	1.95
1	180	100.56	.57	0.00
1	200	101.96	.56	-1.42
1	220	103.17	.56	-2.49
1	240	104.23	.55	-3.31
2	120	89.92	.67	17.28
2	140	93.96	.63	10.07
2	160	96.75	.61	5.82
2	180	98.85	.59	3.01
2	200	100.54	.58	1.02
2	220	101.96	.57	-0.45
2	240	103.92	.55	-3.93
4	120	83.62	.76	32.43
4	140	89.82	.68	18.80
4	160	93.74	.64	11.70
4	170	95.23	.63	9.30
4	180	96.51	.61	7.36
4	190	97.64	.61	5.76
4	200	98.65	.60	4.43
4	240	101.85	.58	0.75
6	120	78.11	.85	48.20
6	140	86.39	.73	26.87
6	160	91.33	.67	16.77
6	180	94.70	.64	10.93
6	200	97.21	.61	7.13
6	220	99.21	.60	4.47
6	240	100.86	.59	2.50
8	120	73.05	.95	65.38
8	140	83.30	.77	34.84
8	160	89.22	.70	21.51
8	180	93.14	.65	14.15
8	200	95.99	.63	9.51
8	220	98.22	.61	6.32
8	240	100.04	.60	4.00
10	120	68.31	1.10	84.40
10	140	80.45	.82	42.90
10	160	87.29	.72	26.09
10	180	91.73	.67	17.18
10	200	94.90	.64	11.70
10	220	97.34	.62	8.01
10	240	99.31	.60	5.35

APPENDIX B. SUMMARY OF TEST CONDITIONS AND TEST RESULTS FOR STACK P10-1
(Fuel Composition: 80.8% H_2; 15.0% CO_2; 1.5% CO and 3.7% H_2O
Hydrogen Utl.: 40%; Air Utl.: 50%)

TEST I.D	VESSEL PRESSURE kPa	CURRENT DENSITY (mA/cm^2)	'MAXIMUM STACK' TEMPERATURE °C	STOICH AIR FLOW	COOLING AIR IN TEMPERATURE (°C)	COOLING AIR ΔT (°C)	COOLING AIR FLOW (SLPM)	STACK AVERAGE* TEMPERATURE (°C)	PEAK TO AVERAGE ΔT (°C)	PRESSURE DROP (mmHg)			AVERAGE POTENTIAL PER CELL (mV)
										ANODE	CATHODE	COOLING	
1A-1	342	100	175	2	141	32.8	2944	174	7	0.93	2.4	0.87	711
1A-2	343	125	174	2	140	27.8	5014	173	8				686
1A-3	342	150	175	2	140	27.2	6440	174	7				665
1A-4	343	175	175	2	139	26.1	8372	172	11				645
1A-5	344	200	175	2	139	23.3	11454	174	8				627
1B-1	342	100	180	2	139	41.7	2714	180	10				712
1B-2	343	150	181	2	140	32.2	5612	179	10				672
1B-3	343	200	181	2	144	26.7	9016	179	10				637
1B-4	342	300	180	2	139	23.88	16514	178	10				571
1B-5	342	250	181	2	139	27.2	12696	179	10	2.2	5.4	8.2	604

*Calculated from experimental thermal profile.

SUMMARY OF TEST CONDITIONS AND TEST RESULTS FOR STACK P10-1 (Cont'd)

TEST I.D	VESSEL PRESSURE kPa	CURRENT DENSITY (mA/cm^2)	'MAXIMUM STACK' TEMPERATURE °C	STOICH AIR FLOW	COOLING AIR IN TEMPERATURE (°C)	COOLING AIR ΔT (°C)	COOLING AIR FLOW (SLPM)	STACK AVERAGE* TEMPERATURE (°C)	PEAK TO AVERAGE ΔT (°C)	PRESSURE DROP (mmHg)			AVERAGE POTENTIAL PER CELL (mV)
										ANODE	CATHODE	COOLING	
1C-1	342	150	190	2	141	47.2	3128	189	13	1.2	2.9	1.0	683
1C-2	343	200	192	2	139	43.9	5382	190	14	1.6	3.8	2.0	649
1C-3	342	250	190	2	139	37.2	8142	187	14	2.3	5.0	3.8	620
1C-4	344	300	191	2	140	34.4	11960	189	12	3.2	6.2	7.2	592
1C-5	344	350	190	2	139	30.0	16836	185	14	4.2	7.6	13.5	558
1D-1	344	150	190	3	144	48.9	2576	190	19				688
1D-2	343	200	190	3	139	46.1	4462	189	17				654
1D-3	343	250	190	3	139	37.8	6946	188	19				623
1D-4	343	300	190	3	141	33.9	10672	188	16				593
1D-5	343	350	190	3	140	30.0	16882	186	15				562

*Calculated from experimental thermal profile.

SUMMARY OF TEST CONDITIONS AND TEST RESULTS FOR STACK P10-1 (Cont'd)

TEST I.D	VESSEL PRESSURE kPa	CURRENT DENSITY (mA/cm^2)	MAXIMUM STACK TEMPERATURE °C	STOICH AIR FLOW	COOLING AIR IN TEMPERATURE (°C)	COOLING AIR ΔT (°C)	COOLING AIR FLOW (SLPM)	STACK AVERAGE* TEMPERATURE (°C)	PEAK TO AVERAGE ΔT (°C)	PRESSURE DROP (mmHg)			AVERAGE POTENTIAL PER CELL (mV)
										ANODE	CATHODE	COOLING	
1E-1	342	100	191	2	150	43.3	2024	189	11				724
1E-2	342	150	190	2	151	33.9	4186	187	10				684
1E-3	342	200	190	2	150	29.4	6854	187	13				651
1E-4	343	225	190	2	150	27.8	9200	187	11				634
1E-5	342	250	190	2	150	27.2	10304	187	13	2.3	5.1	6.1	620
1F-1	342	150	190	2	124	74.4	1840	193	18				687
1F-2	343	200	190	2	125	67.8	2852	191	17				651
1F-3	342	300	191	2	124	51.1	7406	192	18				592
1F-4	343	350	190		125	47.2	10074	191	20				559
1F-5	343	400	190	2	126	40	15594	188	14	5.2	9.0	11.0	528
1F-6	343	350	190	2	126	46.1	9982	189	18				573
2G-1	516	325	190	2	140	31.1	15870	184	11	-	-	-	605

*Calculated from experimental thermal profile.

SUMMARY OF TEST CONDITIONS AND TEST RESULTS FOR STACK P10-1 (Cont'd)

TEST I.D	VESSEL PRESSURE kPa	CURRENT DENSITY (mA/cm^2)	'MAXIMUM STACK' TEMPERATURE °C	STOICH AIR FLOW	COOLING AIR IN TEMPERATURE (°C)	COOLING AIR ΔT (°C)	COOLING AIR FLOW (SLPM)	STACK AVERAGE* TEMPERATURE (°C)	PEAK TO AVERAGE ΔT (°C)	PRESSURE DROP (mmHg)			AVERAGE POTENTIAL PER CELL (mV)
										ANODE	CATHODE	COOLING	
2A-1	516	150	180	2	139	34.4	5060	179	9				701
2A-2	514	200	180	2	140	29.4	7636	178	8				663
2A-3	517	250	180	2	140	32.2	8648	177	8				630
2A-4	514	300	180	2	139	23.3	18584	177	8				597
2A-5	512	300	180	2	141	21.7	19918	177	8				596
2B-1	515	150	190	2	140	52.8	3036	190	13	0.9	1.9	0.56	713
2B-2	517	200	190	2	141	41.7	5014	188	13	1.3	2.5	1.1	679
2B-3	516	300	191	2	138	34.4	12558	186	12	2.4	4.0	5.4	614
2B-4	517	350	190	2	141	28.3	17756	185	12	3.0	4.7	9.8	584
2B-5	511	367	190	2	140	27.8	19964	184	12	3.1	5.0	11.0	574

*Calculated from experimental thermal profile.

SUMMARY OF TEST CONDITIONS AND TEST RESULTS FOR STACK P10-1 (Cont'd)

TEST I.D	VESSEL PRESSURE kPa	CURRENT DENSITY (mA/cm^2)	MAXIMUM STACK TEMPERATURE °C	STOICH AIR FLOW	COOLING AIR IN TEMPERATURE (°C)	COOLING AIR ΔT (°C)	COOLING AIR FLOW (SLPM)	STACK AVERAGE* TEMPERATURE (°C)	PEAK TO AVERAGE ΔT (°C)	PRESSURE DROP (mmHg)			AVERAGE POTENTIAL PER CELL (mV)
										ANODE	CATHODE	COOLING	
2C-1	517	150	190	3	141	51.1	2622	189	18				715
2C-2	516	200	190	3	139	43.3	4462	187	15				681
2C-3	513	300	190	3	142	31.7	11546	86	16				616
2C-4	513	352	190	3	141	31.1	15134	186	17				587
2C-5	513	375	190	3	140	29.4	18354	185	17				572
2D-1	515	100	175	2	140	38.3	1978	175	7				736
2D-2	515	150	176	2	140	28.9	6026	174	7				692
2D-3	519	200	175	2	140	25.6	8694	174	8				654
2D-4	515	250	175	2	140	21.7	14582	173	8				618

Stack was subjected to three pressurization - depressurization cycles.

*Calculated from experimental thermal profile.

SUMMARY OF TEST CONDITIONS AND TEST RESULTS FOR STACK P10-1 (45-Cell)

TEST I.D	VESSEL PRESSURE kPa	CURRENT DENSITY (mA/cm^2)	'MAXIMUM STACK' TEMPERATURE °C	STOICH AIR FLOW	COOLING AIR IN TEMPERATURE (°C)	COOLING AIR ΔT (°C)	COOLING AIR FLOW (SLPM)	STACK AVERAGE* TEMPERATURE (°C)	PEAK TO AVERAGE ΔT (°C)	PRESSURE DROP (mmHg)			AVERAGE POTENTIAL PER CELL (mV)
										ANODE	CATHODE	COOLING	
2E-1	517	150	189	2	150	34.4	5520	188	11				693
2E-2	514	200	191	2	149	30.6	9062	187	10				662
2E-3	518	250	190	2	151	23.3	13478	187	11				629
2E-4	514	284	190	2	N/A	N/A	16100	184	10				607
2F-1	515	150	190	2	124	76.1	1518	191	18				701
2F-2	516	200	190	2	126	60.6	4048	190	21				665
2F-3	516	300	190	2	126	48.3	7774	188	19				597
2F-4	516	350	190	2	124	48.9	10074	188	21				570
2F-5	517	400	190	2	124	38.3	15456	186	20	8.4	11.0	17.5	538

*Calculated from experimental thermal profile.

SUMMARY OF TEST CONDITIONS AND TEST RESULTS FOR STACK P10-1 (45-Cell)

TEST I.D	VESSEL PRESSURE kPa	CURRENT DENSITY (mA/cm^2)	'MAXIMUM STACK' TEMPERATURE °C	STOICH AIR FLOW	COOLING AIR IN TEMPERATURE (°C)	COOLING AIR ΔT (°C)	COOLING AIR FLOW (SLPM)	STACK AVERAGE* TEMPERATURE (°C)	PEAK TO AVERAGE ΔT (°C)	PRESSURE DROP (mmHg)			AVERAGE POTENTIAL PER CELL (mV)
										ANODE	CATHODE	COOLING	
3A-1	688	150	190	2	141	52.8	3404	190	13	1.2-1.8	3.4-3.6	.4-1.2	720
3A-2	687	200	189	2	140	47.8	5014	188	13	.58-.62	1.9-2.0	.6-1.0	687
3A-3	688	300	190	2	139	35.0	11546	187	12	1.6	2.6	3.2-3.6	622
3A-4	689	350	189	2	140	26.7	17940	185	10	2.1	3.2	7.4	592
3B-1	685	150	190	3	142	38.3	2760	190	19				723
3B-2	689	200	191	3	139	50.6	4554	189	21				690
3B-3	687	300	189	3	139	35.0	11270	186	21				625
3B-4	687	350	190	3	141	28.3	16514	186	18				596

SUMMARY OF TEST CONDITIONS AND TEST RESULTS FOR STACK P10-1 (45-Cell)

TEST I.D	VESSEL PRESSURE kPa	CURRENT DENSITY (mA/cm^2)	MAXIMUM STACK TEMPERATURE °C	STOICH AIR FLOW	COOLING AIR IN TEMPERATURE (°C)	COOLING AIR ΔT (°C)	COOLING AIR FLOW (SLPM)	STACK AVERAGE* TEMPERATURE (°C)	PEAK TO AVERAGE ΔT (°C)	PRESSURE DROP (mmHg)			AVERAGE POTENTIAL PER CELL (mV)
										ANODE	CATHODE	COOLING	
3C-1	688	150	190	2	151	37.2	3910	188	7				724
3C-2	685	200	191	2	149	31.1	7590	187	9				689
3C-3	689	250	189	2	151	25.0	12098	186	8				625
3C-4	688	300	190	2	151	21.1	17020	185	8				625
3D-1	688	150	191	2	124	83.9	1886	196	28				728
3D-2	687	200	191	2	125	70.6	3358	191	16				690
3D-3	688	300	190	2	124	50.0	8326	189	17				627
3D-4	687	350	190	2	125	57.8	9430	189	16				595
3D-5	687	400	190	2	125	40.6	14490	187	13	2.7	4.0	5.0	564

*Calculated from experimental thermal profile.

SUMMARY OF TEST CONDITIONS AND TEST RESULTS FOR STACK P10-1 (45-Cell)

TEST I.D	VESSEL PRESSURE kPa	CURRENT DENSITY (mA/cm^2)	'MAXIMUM STACK' TEMPERATURE °C	STOICH AIR FLOW	COOLING AIR IN TEMPERATURE (°C)	COOLING AIR ΔT (°C)	COOLING AIR FLOW (SLPM)	STACK AVERAGE* TEMPERATURE (°C)	PEAK TO AVERAGE ΔT (°C)	PRESSURE DROP (mmHg)			AVERAGE POTENTIAL PER CELL (mV)
										ANODE	CATHODE	COOLING	
3E-1	684	150	180	2	142	33.3	5106	178	9				713
3E-2	686	200	181	2	140	30.6	6900	179	9				670
3E-3	685	250	181	2	140	28.3	11224	178	9				636
3E-4	688	300	181	2	140	22.2	18630	178	9				604
3F-1	688	100	175	2	140	40	3220	176	10				739
3F-2	687	150	175	2	139	33.9	5060	175	7				697
3F-3	689	200	175	2	139	25.6	11132	173	9				660
3G-0001 to 3G-0321	688	325	184	2	140		17204-17250	184	11				602-570

*Calculated from experimental thermal profile.